Copper(II) interacting with the non-steroidal antiinflammatory drug flufenamic acid: Structure, antioxidant activity and binding to DNA and albumins

Copper(II) interacting with the non-steroidal antiinflammatory drug flufenamic acid: Structure, antioxidant activity and binding to DNA and albumins

Charikleia Tolia[a], Athanassios N. Papadopoulos[b], Catherine P. Raptopoulou[c], Vassilis Psycharis[c], Claudio Garino[d], Luca Salassa[e], George Psomas[a,*]

[a] *Department of General and Inorganic Chemistry, Faculty of Chemistry, Aristotle University of Thessaloniki, GR-54124 Thessaloniki, Greece.*
[b] *Department of Nutrition and Dietetics, Faculty of Food Technology and Nutrition, Alexandrion Technological Educational Institution, Sindos, Thessaloniki, Greece.*
[c] *Institute of Advanced Materials, Physicochemical Processes, Nanotechnology & Microsystems, Department of Materials Science, NCSR "Demokritos", GR-15310 Aghia Paraskevi Attikis, Greece.*
[d] *Department of Chemistry and NIS Centre of Excellence, University of Turin, Via P. Giuria 7, 10125 Turin, Italy.*
[e] *CIC biomaGUNE, Paseo Miramón 182, 20009 Donostia–San Sebastian, Spain.*

Abstract

Copper(II) complexes with the non-steroidal antiinflammatory drug flufenamic acid (Hfluf) in the presence of N,N-dimethylformamide (DMF) or nitrogen donor heterocyclic ligands (2,2′-bipyridylamine (bipyam), 1,10-phenanthroline (phen), 2,2′-bipyridine (bipy) or pyridine (py)) have been synthesized and characterized. The crystal structures of $[Cu_2(fluf)_4(DMF)_2]$, **1**, and [Cu(fluf)(bipyam)Cl], **2**, have been determined by X-ray crystallography. Density functional theory (DFT) (CAM-B3LYP/LANL2DZ/6-31G**) was employed to determine the structure of complex **2** and its analogues (complexes [Cu(fluf)(phen)Cl], **3**, [Cu(fluf)(bipy)Cl], **4** and $[Cu(fluf)_2(py)_2]$, **5**). Time-dependent DFT calculations of doublet–doublet transitions show that the lowest-energy band in the absorption spectrum of **2**–**5** has a mixed d–d/LMCT character. UV study of the interaction of the complexes with calf-thymus DNA (CT DNA) has shown that the complexes can bind to CT DNA with [Cu(fluf)(bipy)Cl] exhibiting the highest binding constant to CT DNA. The complexes can bind to CT DNA via intercalation as concluded by studying the cyclic voltammograms of the complexes in the presence of CT DNA solution and by DNA solution viscosity measurements. Competitive studies with ethidium bromide (EB) have shown that the complexes can displace the DNA-bound EB suggesting strong competition with EB. Flufenamic acid and its Cu(II) complexes exhibit good binding affinity to human or bovine serum albumin protein with high binding constant values. All compounds have been tested for their antioxidant and free radical scavenging activity as well as for their in vitro inhibitory activity against soybean lipoxygenase showing significant activity with [Cu(fluf)(phen)Cl] being the most active.

* Corresponding author: Tel.:+30+2310997790; Fax:+30+2310997738; E-mail: gepsomas@chem.auth.gr

1. Introduction

Copper is one of the most important biometals not only because of its role in proteins but also due to its potential synergetic activity with drugs [1,2]. Copper(II) complexes with drugs as ligands exhibiting increased activity in comparison to free drugs have been the subject of many research studies [2–4] and a plethora of copper(II) complexes with diverse ligands showing potential antitumor [5,6], antioxidant [7,8], antibacterial [9–11] and antifungal [12] activity may be found in the literature.

Non-steroidal antiinflammatory drugs (NSAIDs) are the most frequently administrated analgesic, antiinflammatory and antipyretic drugs with known side-effects [13]. In general, the action of NSAIDs is the inhibition of the cyclo-oxygenase (COX)-mediated production of prostaglandins [14]. NSAIDs can also induce the apoptosis of a series of cancer cell lines including colon, breast, prostate, human myeloid leukaemia and stomach cell lines [15] and have a synergistic role in the activity of certain antitumor drugs [16]; these antitumorigenic properties of the NSAIDs may be attributed to COX-independent mechanisms by modulating cell proliferation and cell death in cancer cells lacking COX [17,18], to apoptosis via activation of caspases [19] or via an unknown molecular mechanism where free radicals may also be involved [20,21]. Therefore, in an attempt to investigate the potential anticancer as well as antiinflammatory activity of NSAIDs and their complexes, their interaction with DNA as well as their antioxidant activity should be considered of great importance and further evaluated; it should be noted that only few relevant reports on the interaction of NSAIDs and their complexes with DNA have been published so far [22,23].Furthermore, numerous copper(II) complexes with NSAIDs as ligands have been structurally characterized including those of diclofenac [8,24], diflunisal [25], flufenamic acid [26], ibuprofen [27,28], indomethacin [29], mefenamic acid [7], naproxen [27,28], suprofen [29,30] and tolmentin [27].

Phenylalkanoic acids, anthranilic acids, oxicams, salicylate derivatives, sulfonamides and furanones constitute the chemical classes of NSAIDs [2]. The NSAID flufenamic acid (= Hfluf, Scheme 1) belongs to the derivatives of N-phenylanthranilic acid and resembles chemically to mefenamic and tolfenamic acids and other fenamates in clinical use [31]. Hfluf possesses analgesic, antiinflammatory and antipyretic properties and has been used in musculoskeletal and joint disorders and is administered orally and topically [32]. Its channel-regulating ability [33] has been long known since it has been used as a blocker of calcium-dependent cationic currents [34]. Additionally, Hfluf can inhibit nonselective cation channels [35]. On the other hand, it activates potassium channels [36] and has recently shown an interesting modulatory effect on neuronal sodium channels [32]. The number of the metal complexes of flufenamic acid is rather limited in comparison to other NSAIDs; few copper(II) complexes [26,37] have been found in the literature as well as a zinc complex recently reported by our group [38].

Having in mind the importance of NSAIDs in medicine and the enhanced activity of their metal complexes, we have recently initiated the synthesis, characterization and study of biological activity of Cu(II), Co(II) and Zn(II) with NSAIDs as ligands [7,8,25,31,38–42]. Within this context, we present herein the synthesis of Cu(II) complexes with the NSAID flufenamic acid in the presence of the O-donor ligand N,N-dimethylformamide (DMF) or the nitrogen-donor heterocyclic ligands 2,2′-bipyridylamine (bipyam), 1,10-phenanthroline (phen), 2,2′-bipyridine (bipy) or pyridine (py), resulting in the formation of complexes $[Cu_2(fluf)_4(DMF)_2]$, **1**, [Cu(fluf)(bipyam)Cl], **2**, [Cu(fluf)(phen)Cl], **3**, [Cu(fluf)(bipy)Cl], **4** and $[Cu(fluf)_2(py)_2]$, **5**, respectively. The complexes have been characterized with physicochemical and spectroscopic techniques and their electrochemical behavior has been also investigated. The crystal structures of $[Cu_2(fluf)_4(DMF)_2]$ **1** and [Cu(fluf)(bipyam)Cl] **2** have been determined by X-ray crystallography.

In an attempt to investigate the existence of potential anticancer and/or anti-inflammatory activity of the resultant complexes **1**–**5**, we have focused on (i) the interaction of the complexes with calf-thymus (CT) DNA studied by UV spectroscopy, cyclic voltammetry and viscosity measurements, (ii) the ability of the complexes to displace ethidium bromide (EB) from the EB-DNA complex in order to clarify the existence
of a potential intercalation of the complexes to CT DNA in competition to the classical DNA-intercalator EB studied by fluorescence spectroscopy, (iii) the antioxidant capacity of the complexes by determining their ability to scavenge 1,1-diphenyl-picrylhydrazyl (DPPH), hydroxyl (•OH) and 2,2′-azinobis-(3-ethylbenzothiazoline-6-sulfonic acid) ($ABTS^{\bullet+}$) radicals as well as their inhibitory activity against soybean lipoxygenase (LOX) — since

the use of NSAIDs in medicine as anagelsics and antiinflammatories may be related to free radicals scavenging. Furthermore, the affinity of the complexes to bovine (BSA) and human serum albumin (HSA) has been investigated by fluorescence spectroscopy since binding to such proteins that are involved in the transport of metal ions and metal–drug complexes through the blood stream may result in lower or enhanced biological properties of the original drug, or new paths for drug transportation [43].

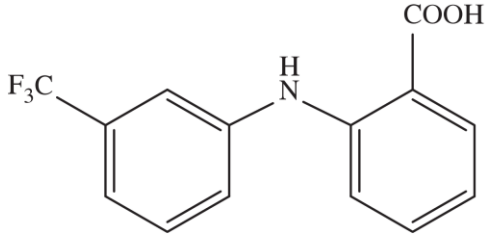

Scheme 1. The NSAID flufenamic acid (=Hfluf).

2. Experimental

2.1. Materials—instrumentation—physical measurements

All chemicals (CuCl2·2H2O, flufenamic acid, bipy, phen, bipyam, py, KOH, CT DNA, BSA, HSA, EB, NaCl and trisodium citrate) were purchased from Sigma-Aldrich Co and all solvents were purchased from Merck. The chemicals and solvents were reagent grade and were used as purchased without any further purification. Tetraethylammonium perchlorate (TEAP) was purchased from Carlo Erba and, prior to its use, it was recrystallized twice from ethanol and dried under vacuum.

DNA stock solution was prepared by dilution of CT DNA to buffer (containing 15 mM trisodium citrate and 150 mM NaCl at pH 7.0) followed by exhaustive stirring for three days, and kept at 4 °C for no longer than a week. The stock solution of CT DNA gave a ratio of UV absorbance at 260 and 280 nm (A_{260}/A_{280}) of 1.89, indicating that the DNA was sufficiently free of protein contamination. The DNA concentration was determined by the UV absorbance at 260 nm after 1:20 dilution using $\varepsilon = 6600\ M^{-1}\ cm^{-1}$ [7,8].

Infrared (IR) spectra (400–4000 cm^{-1}) were recorded on a Nicolet FT-IR 6700 spectrometer with samples prepared as KBr disk. UV–visible (UV–vis) spectra were recorded as nujol mulls and in DMSO solution at concentrations in the range 10^{-5} to 10^{-3} M on a Hitachi U-2001 dual beam spectrophotometer. Room temperature magnetic measurements were carried out on a magnetic susceptibility balance of Sherwood Scientific (Cambridge, UK). C, H and N elemental analysis were performed on a Perkin-Elmer 240B elemental analyzer. Molar conductivity measurements of 1 mM DMSO solution of the complexes were carried out with a Crison Basic 30 conductometer. Fluorescence spectra were recorded in solution on a Hitachi F-7000 fluorescence spectrophotometer. Viscosity experiments were carried out using an ALPHA L Fungilab rotational viscometer equipped with an 18 mL LCP spindle.

Cyclic voltammetry studies were performed on an Eco chemie Autolab Electrochemical analyzer. Cyclic voltammetric experiments were carried out in a 30 mL three-electrode electrolytic cell. The working electrode was platinum disk, a separate Pt single-sheet electrode was used as the counter electrode and a Ag/AgCl electrode saturated with KCl was used as the reference electrode. The cyclic voltammograms of the complexes were recorded in 0.4 mM DMSO solutions and in 0.4 mM 1/2 DMSO/buffer solutions at $\nu = 100\ mV\ s^{-1}$ where TEAP and the buffer solution were the supporting electrolytes, respectively. Oxygen was removed by purging the solutions with pure nitrogen which had been previously saturated with solvent vapors. All electrochemical measurements were performed at 25.0 ± 0.2 °C.

2.2. Synthesis of the complexes

2.2.1. $[Cu_2(fluf)_4(DMF)_2]$, **1**

Potassiumhydroxide (0.4 mmol, 22 mg) was added to a methanolic solution (15 mL) of flufenamic acid (0.4 mmol, 113 mg) and the solution was stirred for 1 h. The solution was added slowly to a methanolic solution (5 mL) of $CuCl_2{\cdot}2H_2O$ (0.2 mmol, 34 mg) followed by the addition of 2 mL of DMF. Dark green crystals of $[Cu_2(fluf)_4(DMF)_2]$ **1** suitable for X-ray structure determination were collected after twenty days. Yield: 90 mg,

65%. Anal. Calcd. for $[Cu_2(fluf)_4(DMF)_2]$ ($C_{62}H_{50}Cu_2F_{12}N_6O_{10}$) (MW = 1394.19): C 54.67, H 3.70, N 6.17; found C 54.25, H 3.59, N 5.95. IR (KBr disk): ν_{max}, cm^{-1}; $\nu(C{=}O)_{DMF}$: 1667 (very strong (vs)); $\nu_{asym}(CO_2)$: 1590 (vs); $\nu_{sym}(CO_2)$: 1400 (vs); $\Delta = \nu_{asym}(CO_2) - \nu_{sym}(CO_2)$ = 190 cm^{-1};UV-vis: λ, nm (ε, M^{-1} cm^{-1}) as nujol mull: 738, 410 (shoulder (sh)), 340, 295; in DMSO: 735 (120), 415 (sh) (150), 335 (14,200), 296 (25,000). μ_{eff} = 1.45 BM. The complex is soluble in DMF and DMSO (Λ_M = 5 mho cm^2 mol^{-1}, in 1 mM DMSO).

2.2.2. [Cu(fluf)(bipyam)Cl], **2**

A methanolic (10 mL) solution containing flufenamic acid (0.2 mmol, 52 mg) and KOH (0.2 mmol, 11 mg) after 1 h stirring was added slowly, and simultaneously with a methanolic solution of bipyam (0.2 mmol, 34 mg), to a methanolic solution (10 mL) of $CuCl_2{\cdot}2H_2O$ (0.2 mmol, 34 mg) and stirred for 15 additional min. Green crystals of [Cu(fluf)(bipyam)Cl] **2** suitable for X-ray structure determination were collected after a week. Yield: 66 mg, 60%. Anal. Calcd. for [Cu(fluf)(bipyam)Cl] ($C_{24}H_{20}ClCuF_3N_4O_2$) (MW = 552.43): C 52.18, H 3.65, N 10.14; found C 52.29, H 3.34, N 10.04. IR (KBr disk): ν_{max}, cm^{-1}; $\nu_{asym}(CO_2)$: 1590 (vs); $\nu_{sym}(CO_2)$: 1410 (vs); Δ = 180 cm^{-1}; UV–vis: λ, nm (ε, M^{-1} cm^{-1}) as nujol mull: 842(sh), 705, 421 (sh), 328, 297; in DMSO: 845 (sh) (15), 702 (105), 420 (sh) (180), 325 (10,300), 300 (13,500). μ_{eff} = 1.98 BM. The complex is soluble in DMF and DMSO (Λ_M = 6 mho cm^2 mol^{-1}, in 1 mM DMSO).

2.2.3. [Cu(fluf)(B)Cl], (B = phen for **3**, bipy for **4**)

Complexes **3** and **4** have been prepared in a similar way to complex **2** with the use of the corresponding N,N′-donor ligand (B), phen (0.2 mmol, 36 mg) for **3** and bipy (0.2 mmol, 31 mg) for **4**. Green microcrystalline product of [Cu(fluf)(phen)Cl] and [Cu(fluf)(bipy)Cl], respectively, was collected after a week.

Data for **3**: Yield: 75 mg, 66%. Anal. Calcd. for ($C_{26}H_{17}ClCuF_3N_3O_2$) (MW = 559.43): C 55.82, H 3.06, N 7.51; found C 55.37, H 2.65, N 8.02. IR (KBr disk): ν_{max}, cm^{-1}; $\nu_{asym}(CO_2)$: 1585 (vs); $\nu_{sym}(CO_2)$: 1395 (vs); Δ = 190 cm^{-1};UV–vis: λ, nm (ε, M^{-1} cm^{-1}) as nujol mull: 852, 710, 414 (sh), 314, 291; in DMSO: 850 (sh) (15), 705 (65), 409 (sh) (175), 312 (7250), 285 (10,500). μ_{eff} = 1.87 BM. The complex is soluble in DMF and DMSO (ΛM = 5 mho cm^2 mol^{-1}, in 1 mM DMSO).

Data for **4**: Yield: 65 mg, 60%. Anal. Calcd. for ($C_{24}H_{17}ClCuF_3N_3O_2$) (MW = 535.41): C 53.84, H 3.20, N 7.85; found C 54.15, H 3.05, N 7.58. IR (KBr disk): ν_{max}, cm^{-1}; $\nu_{asym}(CO_2)$: 1580 (vs); $\nu_{sym}(CO_2)$: 1395 (vs); Δ = 185 cm^{-1};UV–vis: λ, nm (ε, M^{-1} cm^{-1}) as nujol mull: 843 (sh), 704, 408 (sh), 313, 297; in DMSO: 840 (sh) (10), 701 (100), 410 (sh) (190), 315 (12,000), 301 (14,700). μ_{eff} = 1.92 BM. The complex is soluble in DMF and DMSO (Λ_M = 8 mho cm^2 mol^{-1}, in 1 mM DMSO).

2.2.4. $[Cu(fluf)_2(py)_2]$, **5**

Flufenamic acid (0.4 mmol, 113 mg) was dissolved in methanol (10 mL) and KOH (0.4 mmol, 22 mg) was added. After 1 h stirring, the solution was added slowly to a methanolic solution (10 mL) of $CuCl_2{\cdot}2H_2O$ (0.2 mmol, 34 mg) followed by the addition of 2 mL of pyridine. Blue-green microcrystalline product of $[Cu(fluf)_2(py)_2]$ **5** was collected after a month. Yield: 100 mg, 65%. Anal. Calcd. for $[Cu(fluf)_2(py)_2]$ ($C_{38}H_{28}CuF_6N_4O_4$) (MW = 782.20): C 58.35, H 3.61, N 7.16; found C 58.10, H 3.67, N 7.09. IR (KBr disk): ν_{max}, cm_{-1}; $\nu_{asym}(CO_2)$: 1580 (vs); $\nu_{sym}(CO_2)$: 1390 (vs); Δ =190 cm^{-1}; UV–vis: λ, nm (ε, M^{-1} cm^{-1}) as nujol mull: 657, 407 (sh), 341 (sh), 288; in DMSO: 660 (90), 405 (sh) (205), 344 (sh) (8500), 290 (12,500). μ_{eff} = 1.83 BM. The complex is soluble in DMF and DMSO (Λ_M = 5 mho cm^2 mol^{-1}, in 1 mM DMSO).

2.3. X-ray structure determination

A crystal of **1** (0.36 × 0.52 × 0.55 mm) and a crystal of **2** (0.15 × 0.24 × 0.27 mm) were taken from the mother liquor and immediately cooled to −113 °C. Diffraction measurements were made on a Rigaku R-AXIS SPIDER Image Plate diffractometer using graphite monochromated Cu Kα radiation. Data collection (ω-scans) and processing (cell refinement, data reduction and Empirical absorption correction) were performed using the CrystalClear program package [44]. The structures were solved by direct methods using SHELXS-97 [45] and refined by full-matrix least-squares techniques on F^2 with SHELXL-97 [46] (Table 1). Further experimental crystallographic details for **1**: $2\theta_{max}$ = 130°; reflections collected/unique/used, 25717/5057[Rint = 0.0264]/5057; 515 parameters refined; $(\Delta/\sigma)_{max}$ = 0.001; $(\Delta\rho)_{max}/(\Delta\rho)_{min}$ = 0.902/−0.459 e/$Å^3$; R1/wR2 (for all data),

0.0433/0.1100. Further experimental crystallographic details for **2**: $2\theta_{max}$ = 130°; reflections collected/unique/used, 14641/3476[Rint = 0.0275]/3476; 388 parameters refined; $(\Delta/\sigma)_{max}$ = 0.000; $(\Delta\rho)_{max}/(\Delta\rho)_{min}$ = 0.346/−0.344 e/Å^3; R1/wR2 (for all data), 0.0320/0.0737. In both structures, all hydrogen atoms were located by difference maps and were refined isotropically, and all non-hydrogen atoms were refined anisotropically.

Table 1. Crystallographic data for complexes **1** and **2**.

	1	**2**
Formula	$C_{62}H_{50}Cu_2F_{12}N_6O_{10}$	$C_{24}H_{18}ClCuF_3N_4O_2$
Fw	1394.16	550.41
T (K)	160(2)	160(2)
Crystal system	Monoclinic	Triclinic
Space group	P $2_{1/n}$	P -1
a (Å)	12.7379(2)	8.5858(1)
b (Å)	9.0968(2)	9.0373(1)
c (Å)	26.8191(5)	14.9190(2)
α (^{o})	90.00	77.038(1)
β (^{o})	104.168(1)	76.198(1)
γ (^{o})	90.00	82.703(1)
Volume (Å^3)	3013.11(10)	1092.22(2)
Z	2	2
D(calc), Mg m^{-3}	1.537	1.674
Abs. coef., μ, mm^{-1}	1.766	3.053
GOF on F^2	1.019	1.038
R1=	0.0403 [a]	0.0292 [b]
wR2=	0.1078 [a]	0.0722 [b]

[a] 4618 reflections with I > 2σ(I); [b]3193 reflections with I > 2σ(I)

2.4. Computational studies

All calculations on complexes **2**–**5** were performed with the Gaussian 09 (G09) program [47] employing the density functional theory (DFT) and time-dependent density functional theory (TD-DFT) methods [48,49]. The hybrid CAM-B3LYP [50], functional was used in combination with the LANL2DZ ECP [51] (for Cu) and with the 6–31 G** basis set (for all other atoms) [52]. Thirty-two low-lying excitation energies with the corresponding oscillator strengths were determined for **2**–**5** at the ground-state geometry by TD-DFT. The PCM solvent model [53] was adopted in the TD-DFT calculations with DMSO as solvent. Theoretical UV–Vis spectra were obtained using GAUSSSUM 2.2 [54]. Molecular graphics images were produced using the UCSF Chimera package from the Resource for Biocomputing, Visualization, and Informatics at the University of California, San Francisco (supported by NIH P41 RR001081) [55].

2.5. Albumin binding studies

The protein binding study was performed by tryptophan fluorescence quenching experiments using BSA (3 μM) or HSA (3 μM) in buffer (containing 15 mM trisodium citrate and 150 mM NaCl at pH 7.0). The quenching of the emission intensity of tryptophan residues of BSA at 342 nm or HSA at 351 nm was monitored using Hfluf and complexes **1**–**5** as quenchers with increasing concentration (up to 2.2 × 10^{-5} M) [56] and the fluorescence spectra were recorded from 300 to 500 nm at an excitation wavelength of 296 nm. The fluorescence spectra of the compounds recorded under the same experimental conditions exhibited a maximum emission at 374 nm. Therefore, the quantitative studies of the serum albumin fluorescence spectra were performed after their correction by subtracting the spectra of the compounds. The Stern–Volmer and Scatchard equations and graphs have been used in order to study the interaction of a quencher with serum albumins. The values of the dynamic quenching constant (K_{SV}, M^{-1}) and the quenching constant (k_q, M^{-1} s^{-1}) for the interaction of Hfluf and complexes **1**–**5** with SA have been derived from the Stern–Volmer quenching equation [57]:

$$\frac{I_0}{I} = 1 + k_q \tau_q [Q] = 1 + K_{SV}[Q] \qquad (1)$$

where Io = the initial tryptophan fluorescence intensity of SA, I = the tryptophan fluorescence intensity of SA after the addition of the quencher, k_q = the quenching rate constants of SA, K_{SV} = the dynamic quenching constant, τ_o = the average lifetime of SA without the quencher, [Q] = the concentration of the quencher respectively, $K_{SV} = k_q \tau_o$ and, taking as fluorescence lifetime (τ_o) of tryptophan in SA at around 10^{-8} s [57], K_{SV} (in M^{-1}) can be obtained by the slope of the diagram Io/I vs [Q], and subsequently the approximate k_q (in M^{-1} s^{-1}) may be calculated.

From the application of the Scatchard [58] equation:

$$\frac{\Delta I/_{Io}}{[Q]} = nK - k\frac{\Delta I}{Io} \qquad (2)$$

the association binding constant K (in M^{-1}) may be calculated from the slope in the Scatchard plots $\frac{\Delta I/_{Io}}{[Q]}$ versus ΔI/Io and the number of binding sites per albumin (n) is given by the ratio of y intercept to the slope [58].

2.6. DNA-binding studies

The interaction of Hfluf and complexes **1**–**5** with CT DNA has been studied with UV spectroscopy in order to investigate the possible binding modes to CT DNA and to calculate the binding constants to CT DNA (Kb). The UV spectra of CT DNA have been recorded for a constant CT DNA concentration in the presence of each compound at diverse r (=[compound]/[CT DNA] mixing ratios) values. The binding constants, K_b, of the complexes with CT DNA have been determined using the UV spectra of the compound recorded for a constant concentration in the absence or presence of CT DNA for diverse r values. Control experiments with DMSO were performed and no changes in the spectra of CT DNA were observed. The binding constant of the complexes with CT DNA, K_b, is used in order to estimate the magnitude of the binding strength of their interaction. K_b (in M^{-1}) can be calculated by the ratio of slope to the y intercept in plots $\frac{[DNA]}{(\varepsilon_A - \varepsilon_f)}$ versus [DNA], according to the equation [59]:

$$\frac{[DNA]}{(\varepsilon_A - \varepsilon_f)} = \frac{[DNA]}{(\varepsilon_b - \varepsilon_f)} + \frac{1}{K_b(\varepsilon_b - \varepsilon_f)} \qquad (3)$$

where [DNA] is the concentration of DNA in base pairs, ε_f is the extinction coefficient for the free complex at the corresponding λ_{max}, $\varepsilon_A = A_{obsd}/[complex]$ and ε_b is the extinction coefficient for the complex in the fully bound form.

The interaction of complexes **1**–**5** with CT DNA has been also investigated by monitoring the changes observed in the cyclic voltammogramof a 0.40 mM1:2 DMSO:buffer solution of complex upon addition of CT DNA at diverse r values. The buffer was also used as the supporting electrolyte and the cyclic voltammograms were recorded at $\nu = 100$ mV s^{-1}.

Viscosity experiments were carried out using an ALPHA L Fungilab rotational viscometer equipped with an 18 mL LCP spindle and the measurements were performed at 100 rpm. The viscosity of a DNA solution has been measured in the presence of increasing amounts of the compounds. The relation between the relative solution viscosity (η/η_0) and DNA length (L/L_0) is given by the equation $L/L_0 = (\eta/\eta_0)^{1/3}$, where L_0 denotes the apparent molecular length in the absence of the compound. The obtained data are presented as $(\eta/\eta_0)^{1/3}$ versus r, where η is the viscosity of DNA in the presence of a complex, and η_0 is the viscosity of DNA alone in buffer solution.

The competitive studies of each compound with EB have been investigated with fluorescence spectroscopy in order to examine whether the compound can displace EB from its CT DNA–EB complex. The CT DNA–EB complex was prepared by adding 20 μM EB and 26 μM CT DNA in buffer (150 mM NaCl and 15 mM trisodium citrate at pH 7.0). The possible intercalating effect of the compounds was studied by adding a certain amount of a solution of the compound step by step into a solution of the DNA–EB complex. The influence of the addition of each compound to the DNA–EB complex solution has been obtained by recording the variation of fluorescence emission spectra. Flufenamic acid and its complexes **1**–**5** show no fluorescence at room temperature

in solution or in the presence of CT DNA under the same experimental conditions; therefore, the observed quenching is attributed to the displacement of EB from its EB–DNA complex. The Stern–Volmer plots of DNA–EB have been used in order to study the quenching of EB bound to DNA by the compounds according to the linear Stern–Volmer equation:

$$\frac{Io}{I} = 1 + K_{SV}[Q] \qquad (4)$$

where Io and I are the emission intensities in the absence and the presence of the quencher, respectively, [Q] is the concentration of the quencher (Hfluf or complexes 1–5) [7,60]. The values of the Stern–Volmer constant (K_{SV}, in M^{-1}) are obtained by the slope of the diagram Io/I vs [Q].

2.7. Antioxidant biological assay

In the in vitro assays each experiment was performed at least in triplicate and the standard deviation of absorbance was less than 10% of the mean.

2.7.1. Determination of the reducing activity of the stable radical

1,1-diphenyl-picrylhydrazyl (DPPH) To a solution of DPPH (0.1 mM) in absolute ethanol an equal volume of the compounds dissolved in ethanol was added. As control solution ethanol was used. The concentration of the solution of the compounds was 0.1 mM. The absorbance at 517 nm was recorded at room temperature, after 20 and 60 min in order to examine the time-dependence of the radical scavenging activity [7,61]. The radical scavenging activity of the compounds was expressed as the percentage inhibition of the absorbance of the initial DPPH solution (RA%). NDGA (nordihydroguaiaretic acid) and BHT (butylated hydroxytoluene) were used as reference compounds.

2.7.2. Competition of the tested compoundswith DMSO for hydroxyl radicals

The hydroxyl radicals generated by the Fe^{3+}/ascorbic acid system, were detected according to Nash [7,61], by the determination of formaldehyde produced from the oxidation of DMSO. The reaction mixture contained EDTA (0.1 mM), Fe^{3+} (167 μM), DMSO (33 mM) in phosphate buffer (50 mM, pH 7.4), the tested compounds (concentration 0.1 mM) and ascorbic acid (10 mM). After 30 min of incubation (37 °C) the reaction was stopped with CCl_3COOH (17% w/v) and the absorbance at λ = 412 nm was measured. Trolox was used as an appropriate standard. The competition of the compounds with DMSO for OH•, generated by the Fe^{3+}/ascorbic acid system, expressed as percent inhibition of formaldehyde production,was used for the evaluation of their hydroxyl radical scavenging activity (•OH%).

2.7.3. Assay of radical cation scavenging activity

ABTS was dissolved in water to a 2 mM concentration. ABTS radical cation ($ABTS^{\bullet+}$) was produced by reacting ABTS stock solution with 0.17 mM potassium persulfate and allowing the mixture to stand in the dark at room temperature for 12–16 h before use. Because ABTS and potassium persulfate react stoichiometrically at a ratio of 1:0.5, this will result in incomplete oxidation of the ABTS. Oxidation of the ABTS commenced immediately, but the absorbance was not maximal and stable until more than 6 h had elapsed. The radical was stable in this form for more than 2 days when stored in the dark at room temperature. The $ABTS^{\bullet+}$ solution was diluted with ethanol to an absorbance of 0.70 at 734 nm. After addition of 10 μL of diluted compounds or standards (0.1 mM) in DMSO, the absorbance reading was taken exactly 1 min after initial mixing [62,63]. The radical scavenging activity of the complexes was expressed as the percentage inhibition of the absorbance of the initial ABTS solution (ABTS%). Trolox was used as an appropriate standard.

2.7.4. Soybean lipoxygenase inhibition study in vitro

The in vitro study was evaluated as reported previously [61].The tested compounds dissolved in ethanol were incubated at room temperature with sodium linoleate (0.1 mM) and 0.2 cm^3 of enzyme solution ($1/9 \times 10^{-4}$ w/v in saline). The conversion of sodium linoleate to 13-hydroperoxylinoleic acid at 234 nm was recorded and compared with the appropriate standard inhibitor caffeic acid.

3. Results and discussion

3.1. Synthesis and spectroscopic study

The structurally characterized complexes have been synthesized in high yield via the reaction of the NSAID Hfluf with KOH, $CuCl_2{\cdot}2H_2O$ and the corresponding O-(DMF, Eq. (5)) for **1**, or N,N′-donor, e.g. (bipyam, Eq. (6)) for **2**, according to the equations:

$$2CuCl_2{\cdot}2H_2O + 4Hfluf + 4KOH + 2DMF \rightarrow [Cu_2(fluf)_4(DMF)_2] + 4KCl + 8H_2O \quad (5)$$

$$CuCl_2{\cdot}2H_2O + Hfluf + KOH + bipyam \rightarrow [Cu(fluf)(bipyam)Cl] + KCl\ 3H_2O \quad (6)$$

IR spectroscopy has been used in order to confirm the deprotonation and binding mode of flufenamic acid. In the IR spectrum of Hfluf, the absorption band at 3436 (br (broad), m (medium)) cm^{-1} attributed to the ν(H–O) stretching vibration has disappeared upon binding to the metal ion, revealing the deprotonation of the carboxylate group. The bands at 1655 (s (strong)) cm^{-1} and 1255(s) cm^{-1} attributed to the stretching vibrations $\nu(C{=}O)_{carboxylic}$ and $\nu(C{-}O)_{carboxylic}$ of the carboxylic moiety (–COOH), respectively, have shifted in the IR spectra of complexes **1**–**5** in the range of 1580–1590 cm^{-1} and 1390–1401 cm^{-1} assigned to antisymmetric, $\nu_{asym}(CO_2)$, and symmetric, $\nu_{sym}(CO_2)$, stretching vibrations of the carboxylato group, respectively. The difference Δ $[=\nu_{asym}(CO_2)-\nu_{sym}(CO_2)]$ is a characteristic tool for determining the coordination mode of the carboxylate ligands and has a value falling in the range of 180–190 cm^{-1} indicative of bidentate binding mode of the flufenamato ligand [38,64].

In the visible region, complexes **2**–**4** exhibit a d–d transition band in the range of 700–705 nm (ε = 65–100 M^{-1} cm^{-1}) and an additional weak broad d–d transition band at 840–850 nm (ε = 10–15 M^{-1} cm^{-1}), typical for distorted square pyramidal geometry [65]. For complexes **1** and **5**, a low-intensity band with ε =90–120 M^{-1} cm^{-1} observed in the Vis region (735 nm (ε = 120 M^{-1} cm^{-1}) and 660 nm (ε = 90 M^{-1} cm^{-1}), respectively) can be assigned to a $^2E_g \rightarrow {}^2T_{2g}$ d–d transition, typical for Cu(II) complexes with octahedral local symmetry. The complexes also exhibit a shoulder, at 405–420 nm (ε = 150–205 M^{-1} cm^{-1}) which may be assigned to a charge-transfer transition. Similar spectroscopic features have been reported for the Cu(II) complexes with the NSAIDs diflunisal, naproxen and diclofenac [8,25]. Time-dependent DFT calculations were performed on the optimized complexes **2**–**5** to confirm such assignment. Fig. 1(A) shows vertical electronic transitions and the resulting theoretical spectrum in the case of complex **2**. The electron density difference maps (EDDMs) reported (Fig. 1(B)) can be used to visualize the nature of selected transitions. EDDMs highlight that the lowest-energy band is prevalently composed by ligand-to-metal charge transfer (LMCT) transitions (although some d–d character is present), while the band at ~400 nm is a mixed d–d/LMCT. Similar results are obtained for the other compounds (Tables S1–S4 and Figs. S1–S3) with **3** and **4** showing a more pronounced d–d character in the lowest-energy states.

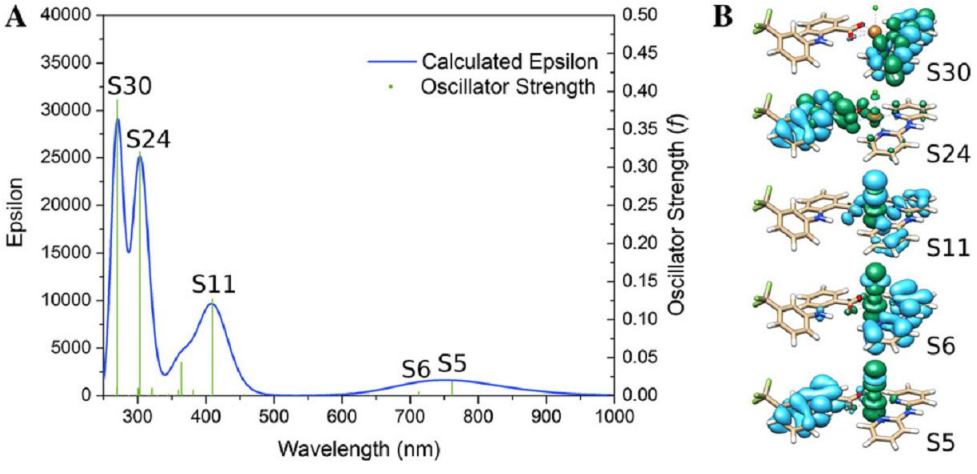

Fig. 1. (A) Theoretical absorption spectra for **2** in DMSO at the CAM-B3LYP/LANL2DZ/6-31 G** level. Doublet-doublet transitions are shown as vertical bars with heights equal to their oscillator strengths. The theoretical curves were obtained using GAUSSSUM 2.2 [54]; (B) Selected EDDMs for **2**, light blue indicates a decrease in electron density, while green indicates an increase.

The UV spectra of the complexes have been also recorded in the pH range of 6–8 (since the biological experiments are performed at pH = 7) with the use of diverse buffer solutions (150 mM NaCl and 15 mM trisodium citrate at pH values regulated by HCl solution) without showing (data not shown) any significant changes (shift of the λ_{max} or new peaks), indicating that the complexes are stable in the pH range = 6–8. The fact that complexes 1–5 have the same UV–Vis spectral pattern in nujol and in DMSO solution as well as in the presence of the buffer solution (150 mM NaCl and 15 mM trisodium citrate in the pH 7.0) used in the biological experiments and in the pH range = 6–8 in combination to non-dissociation in DMSO solution ($\Lambda_M \leq 8$ mho cm^2 mol^{-1}, in 1 mM DMSO solution) suggests that the compounds keep their integrity in solution [38,66].

The μ_{eff} value for **1** (= 1.45 BM) is typical for dinuclear copper(II) complexes with a paddle-wheel arrangement, in agreement with μ_{eff} values of diclofenac [24], diflunisal [25] and naproxen [27] structurally analogous Cu(II) complexes. The observed values of μ_{eff} (= 1.83–1.98 BM) for complexes **2**–**5** are higher than the spin-only value (= 1.73 BM) at room temperature and typical for mononuclear Cu(II) complexes with d^9 configuration (S = 1/2) [7,67]. Spin density surfaces calculated with the DFT method (Fig. 2 and Tables S5–S9) are in agreement with such assignment.

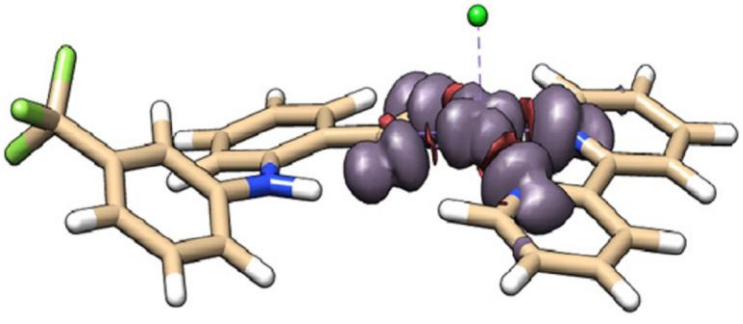

Fig. 2. Spin density surface for complex **4** calculated in DMSO at the CAM-B3LYP/LANL2DZ/6-31 G** level using the PCM solvent (DMSO) method.

3.2. Structure of the complexes

3.2.1. Crystal structure of $[Cu_2(fluf)_4(DMF)_2]$ **1**

The crystal structure of complex 1 is composed of centrosymmetric dimers. The molecular structure of the complex appears in Fig. 3, and selected bond distances and angles are given in Table 2.

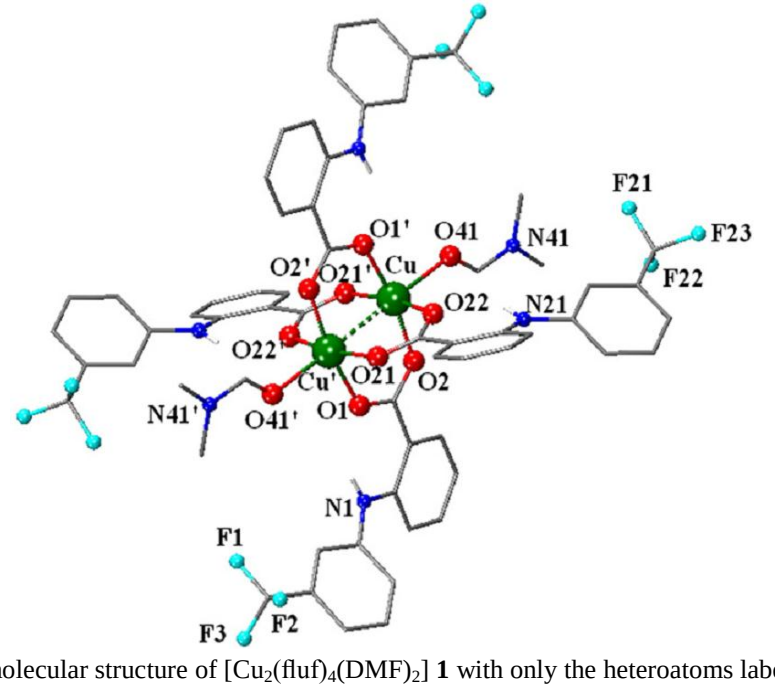

Fig. 3. A drawing of the molecular structure of $[Cu_2(fluf)_4(DMF)_2]$ **1** with only the heteroatoms labeling.

Table 2. Selected bond distances and angles for complex $[Cu_2(fluf)_4(dmf)_2]$.

Bond distances	**(Å)**		
Cu–O(1')	1.968(2)	Cu–O(2)	1.964(2)
Cu–O(21')	1.961(2)	Cu–O(41)	2.131(2)
Cu–O(22)	1.972(2)	Cu…Cu'	2.618(1)
O(1)–C(1)	1.268(3)	C(21)–O(21)	1.257(3)
O(2)–C(1)	1.263(3)	C(21)–O(22)	1.265(3)
Bond angles	**(°)**		
O(1')–Cu–O(2)	168.64(7)	O(2)–Cu–O(21')	88.45(7)
O(1')–Cu–O(21')	89.38(8)	O(2)–Cu–O(22)	90.29(7)
O(1')–Cu–O(22)	89.64(7)	O(2)–Cu–O(41)	100.10(7)
O(1')–Cu–O(41)	91.22(7)	O(21')–Cu–O(22)	168.60(7)
O(22)–Cu–O(41)	94.70(6)	O(21')–Cu–O(41)	96.68(7)

Primed atoms are generated by symmetry: (') 1–x, 1–y, 1–z.

Four bidentate flufenamato ligands form syn-syn carboxylate bridges between isolated pairs of copper atoms separated by 2.618(1) Å, distance lying in the range observed for dinuclear copper(II) complexes of the formula $[Cu_2(O_2CR)_2(L)_2]$ (R = Me, $ClCH_2$, Et, C_5H_{11}, C_6H_{13}, C_8H_{17},4-HOC_6H_4, H, FCH_2 or Ph; L = O-donor (DMSO, DMF, methanol, H_2O) or N-donor (py, urea, quinoline, methylpyridine or nicotinamide) ligand) [25] with a paddlewheel structural motif.

The $Cu–O_{carb}$ distances are quite similar and range from 1.961(2) to 1.972(2) Å. The sum of all interatomic distances in the CuO_5 chromophore (½ of Cu···Cu distance = 1.309 Å is included) 11.305 Å is close to 11.348 Å, average sum for a series of copper(II) binuclear carboxylate compounds [25]. The bridging path lengths (Cu–O(1)–C(1)–O(2)–Cu′ = 6.463 Å and Cu–O(21)–C(21)–O(22)–Cu′ = 6.455 Å) are within the range observed for copper(II) carboxylate dimers. The copper atom is displaced 0.195 Å toward the DMF ligand from the plane containing the four co-ordinated carboxylato oxygen atoms and is in the range of 0.19–0.22 Å known for binuclear carboxylate complexes [25].

Assuming a five-coordinate copper chromophore, each copper atom could be described as having a square pyramidal geometry. The tetragonality [67] T^5 = 0.923, based on the changes in bond lengths, along with the trigonality index [68] [$\tau = (\varphi_1 - \varphi_2)/60°$, where φ_1 and φ_2 are the largest angles in the coordination sphere; τ = 0 for a perfect square pyramid, and τ = 1 for a perfect trigonal bipyramid] τ = (168.64–168.60)/60 = 0.00°, show no distortion from the regular square-based pyramidal geometry.

Among the Cu(II)–NSAIDs complexes that have been structurally characterized, **1** has similar structure with $[Cu_2(nap)_4(DMSO)_2]$ [27], $[Cu_2(dicl)_4(DMF)_2]$ [24], $[Cu_2(dicl)_4(acetone)_2]$ [69] and $[Cu_2(difl)_4(DMF)_2]$ [25], where Hnap = naproxen, Nadicl = sodium diclofenac and Hdifl =diflunisal are NSAIDs. The dimers in **1** are stabilized via four intra-molecular hydrogen bonding interactions developed within the four flufenamato ligands [N(1)···O(1) = 2.653 Å, H(1)N···O(1) = 2.057 Å, N(1)–H(1)N···O(1) = 134.9°; N(21)···O(22) = 2.662 Å, H(21)N···O(22) = 2.045 Å, N(21)–H(21)N···O(22) =136.0°].

3.2.2. Crystal structure of [Cu(fluf)(bipyam)Cl]

In [Cu(fluf)(bipyam)Cl], **2**, thedeprotonated flufenamato is coordinated to copper atom via the two carboxylato oxygen atoms on bidentate asymmetric chelating mode (C(1)–O(1) = 1.269(2) Å and C(1)–O(2) = 1.278(2) Å). A diagram of complex **2** and the dimers formed in the structure are shown in Fig. 4, and selected bond distances and angles are listed in Table 3.

The copper atom is five-coordinate and could be described possessing a slightly distorted square pyramidal geometry. The tetragonality T^5 = 0.803 [67], along with the trigonality index τ = (155.44°–155.38°)/60° = 0.001 [68], show slight distortion from the regular square-based pyramidal geometry. The chelate rings formed by nitrogen atoms N(11) and N(12) [Cu(1)–N(11) = 1.967(2) Å and Cu(1)–N(12) = 1.959(2) Å] of the bipyam ligand (i.e. the six-membered ring Cu–N–C–N–C–N) and by the carboxylate oxygen atoms O(1) and O(2) [Cu(1)–O(1) = 2.029(2) Å and Cu(1–O(2) = 2.036(1) Å] (i.e. the four-membered ring Cu–O–C–O) of the flufenamato ligand possess the basal plane, while the Cl atom [Cu(1)–Cl = 2.488(1) Å] occupies the apical

position. The values of all bond lengths and angles mentioned above are very close to the corresponding values for five-coordinate Cu atoms in distorted square pyramidal geometry with Cl in apical position and chelating bipyam and various carboxylato ligands in the basal plane [70–77].

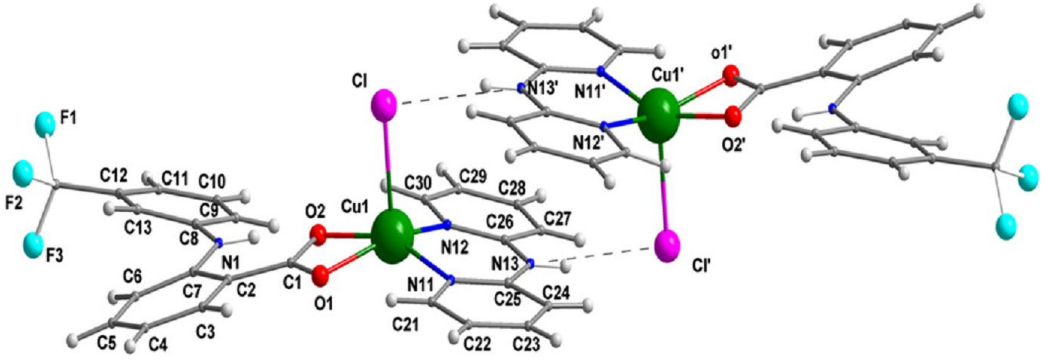

Fig. 4. Dimers of clusters formed through hydrogen bonds and numbering scheme for the symmetry independent complex in the unit cell of 2. Symmetry code: (′):-x,-y,-z.

Table 3. Selected bond distances and angles for [Cu(fluf)(bipyam)Cl] **2.**

Bond distances	**(Å)**		
Cu(1)–O(1)	2.029(2)	Cu(1)–N(11)	1.967(2)
Cu(1)–O(2)	2.036(1)	Cu(1)–N(12)	1.959(2)
Cu(1)–Cl	2.488(1)	C(1)–O(2)	1.278(3)
C(1)–O(1)	1.269(2)		
Bond angles	**(°)**		
O(1)–Cu(1)–O(2)	64.58(6)	O(2)–Cu(1)–N(11)	155.44(8)
O(1)–Cu(1)–N(11)	97.70(7)	O(2)–Cu(1)–N(12)	96.87(6)
O(1)–Cu(1)–N(12)	155.38(8)	O(2)–Cu(1)–Cl	97.20(5)
O(1)–Cu(1)–Cl	95.34(5)	N(12)–Cu(1)–Cl	103.41(6)
N(11)–Cu(1)–N(12)	94.16(7)	N(11)–Cu(1)–Cl	101.48(6)

The copper atom is displaced 0.336 Å from the basal plane towards the chloro ligand which is 2.818 Å away from the mean basal plane. The trans atoms system of the basal plane gives angles of O(1)–Cu(1)–N(12) = 155.38(8)° and O(2)–Cu(1)–N(11) = 155.44(8)°. The observed N(11)\Cu(1)\N(12) bite angle of bipyam (94.16(7)°) and those of the chelating atoms to Cu (Table 3) fall in the range of angles found in similar complexes [70–77]. An interesting feature concerns the bite angle values and planarity of bipyam chelating ligand with respect to the ligands completing the coordination sphere of Cu ion. The N–Cu–N chelating angle in **2** is higher than the corresponding angle (91.96(7)°) in distorted octahedral CuN_2O_4 environment [7] and in distorted square pyramidal $CuClN_2O_2$ environment (91.98° [78] and 90.50° [79]). This reduction in the values of N\Cu\N chelate angle is probably related to the deviation of bipyam ligands from planarity. In the complexes studied in references [78,79] the bipyam ligands are not planar and the puckering of the molecule is defined by the angle of the planar pyridine rings of the bipyam ligands [73]. Puckering probably results from the stereochemical interaction developed between bipyam ligands and the oxygen atoms of other ligands completing the coordination sphere of copper atoms, which in both of the latter cases is CuN_2O_2Cl distorted square pyramidal as in **2**. In both of these cases the chelating oxygens participate in five-membered rings and the bite angles are 81.65° and 81.84° respectively, significantly greater than the analogous O–Cu–O bite angle in **2** (Table 3), which is formed by oxygen atoms participating in four-membered rings. In **2**, the angle between the planar pyridine rings of the bipyam ligands is 5.80°, slightly larger than those in complexes studied in [70,71,73–76] which are lower than 4.0°. For the complexes studied in [72] and [77], this angle takes the values 12.20° and 9.06° respectively. In the cases studied in [78] and [79] where the chelating oxygen atoms participate in five-membered rings the bending angles take significantly higher values, 20.19° and 31.30°, respectively.

The molecules of **2** are stabilized through an intra-molecular hydrogen bonding interaction within the flufenamato ligand [N(1)···O(2) = 2.667 Å, H(1)N···O(1) = 1.971 Å, N(1)–H(1)N···O(1) = 143.2°], whereas they form dimers through two inter-molecular hydrogen bonds involving the NH moiety of bipyam and the chloro ligand [N(13)···Cl (−x, −y, −z) = 3.159 Å, H(13)N···Cl = 2.363 Å, N(13)–H(13)N···Cl = 167.0°] resulting in a face to face stacking of bipyam ligands belonging to neighboring centrosymmetrically related complexes (Fig. 4). The interplanar distance of bipyam ligand plane is 3.286 Å a value close to the one (3.341 Å) observed in [76].These type of hydrogen bond interactions are observed for neighboring complexes with formula [Cu(II)(bipyam)(RCO_2)Cl] studied in [70–72]. With the exception of those studied in [72] and [77], all the other complexes form dimers of the type observed in **2**.

3.2.3. Proposed structures of complexes **3–5**

Based on IR, UV–Vis and magnetic measurements data, complexes **3**–**5** are also mononuclear with the deprotonated flufenamato ligands bound to copper ion via the carboxylato oxygen atoms. From the UV–Vis spectra a distorted square pyramidal environment around copper may be suggested for complexes 3 and 4 which are expected to have crystal structure similar to that of complex 2, with the two oxygen atoms of flufenamato ligand and the two nitrogen atoms of the 1,10-phenanthroline or 2,2´-bipyridine ligand forming the basis of the pyramid and the chlorine atom lying at the apex. On the other hand, for complex **5** a distorted octahedron geometry of copper may be suggested (the octahedron is formed by four oxygen atoms of the two flufenamato ligands and two nitrogen atoms provided by two pyridine ligands) and is similar to that of [Cu(diflunisal)$_2$(py)$_2$] [25] and [Cu(diclofenac)$_2$(py)$_2$] [8] (Nadicl the NSAID sodium diclofenac) which also exhibit a distorted octahedral arrangement around Cu(II) atom and their structures are available in the literature.

DFT geometry optimization calculation were performed at the CAM-B3LYP/LANL2DZ/6-31G** level to obtain structural insights on **3**–**5**. Selected bond distances (Å) and angles (°) (including complex **2**) are reported in Table 4 and confirm spectroscopic observations.

Table 4. Selected bond distances (Å) and angles (°) for the DFT-calculated structure of **2-5** at the CAM-B3LYP/LANL2DZ/6-31G** level using the PCM solvent (DMSO) method.

	2	**3**	**4**	**5**	
Bond distances					
Cu(1)–O(1)	2.015	2.005	1.998	Cu(1)–O(1)	1.978
Cu(1)–O(2)	2.054	2.029	2.041	Cu(1)–O(2)	2.570
Cu(1)–Cl	2.050	2.483	2.483	Cu(1)–N(1)	2.046
Cu(1)–N(11)	2.015	2.035	2.019	Cu(1)–O(4)	1.981
Cu(1)–N(12)	2.006	2.034	2.013	Cu(1)–O(5)	2.554
C(1)–O(1)	1.273	1.274	1.275	Cu(1)–N(2)	2.057
C(1)–O(2)	1.280	1.281	1.280		
Angles (°)					
O(1)–Cu(1)–O(2)	64.4	65.2	65.1	O(1)–Cu(1)–O(2)	56.3
O(1)–Cu(1)–N(11)	97.3	100.8	100.7	O(1)–Cu(1)–O(3)	179.4
O(1)–Cu(1)–N(12)	156.5	156.3	157.7	O(1)–Cu(1)–O(4)	122.8
O(1)–Cu(1)–Cl	100.7	102.1	101.5	O(1)-Cu(1)–N(1)	90.1
N(11)–Cu(1)–N(12)	91.8	81.9	80.9	O(1)–Cu(1)–N(2)	90.0
O(2)–Cu(1)–N(11)	153.2	154.2	152.7	O(2)–Cu(1)–O(3)	124.2
O(2)–Cu(1)–N(12)	98.9	102.5	103.6	O(2)–Cu(1)–O(4)	177.2
O(2)–Cu(1)–Cl	101.4	102.2	102.1	O(2)–Cu(1)–N(1)	91.3
N(12)–Cu(1)–Cl	101.1	100.3	99.7	O(2)–Cu(1)–N(2)	88.3
N(11)–Cu(1)–Cl	98.7	101.9	103.6	O(3)–Cu(1)–O(4)	56.6
				O(3)–Cu(1)–N(1)	90.12
				O(3)–Cu(1)–N(2)	89.7
				O(4)–Cu(1)–N(1)	91.4
				O(4)–Cu(1)–N(2)	89.4
				N(1)–Cu(1)–N(2)	179.4

3.3. Interaction of the complexes with serum albumins

Serumalbumin (SA), the most abundant protein in plasma, is mainly involved in the transport of metal ions, drugs and their metal complexes through the blood stream [80]. Human serum albumin (HSA) has a tryptophan located at position 214, while bovine serum albumin (BSA), the most extensively studied serum albumin due to its structural homology with HSA, has two tryptophans, Trp-134 and Trp-212 [81]. BSA and HSA solutions exhibit an intense fluorescence emission with $\lambda_{em,max}$ = 342 nm and 351 nm, respectively, due to the tryptophan residues, when excited at 295 nm [56]. Hfluf and its complexes **1**–**5** exhibit a maximum emission at 374 nm under the same experimental conditions; therefore the changes and the quenching occurring in the BSA or HSA fluorescence emission spectra upon addition of Hfluf or complexes **1**–**5** at 343 nm and 351 nm, respectively, are primarily due to change in protein conformation, subunit association, substrate binding or denaturation [81].

Addition of Hfluf and complexes **1**–**5** to SA solution results in moderate to significant quenching of HSA fluorescence at λ = 351 nm (Fig. 5(A)) (quenching up to 89% of the initial fluorescence intensity for **1**) and to a much more enhanced quenching of the BSA fluorescence at λ = 343 nm (Fig. 5(B)) (quenching up to 99% of the initial fluorescence intensity for **1**). The observed quenching may be due to possible changes in protein secondary structure leading to changes in tryptophan environment of HSA, and thus indicating the binding of each complex to the albumins [82].

The K_{sv} and k_q values for Hfluf and complexes **1**–**5** interacting with albumins have been calculated with Stern–Volmer quenching equation (Eq. (1)) and Stern–Volmer plots (Figs. S4 and 5), are given in Table 5 and indicate good quenching ability of the compounds with **1** exhibiting the strongest quenching ability (kq = 3.79(±0.32) × 10^{13} M^{-1} s^{-1} for HSA and 5.07(±0.74) × 1014 M^{-1} s^{-1} for BSA). The k_q values (>10^{12} M^{-1} s^{-1}) are higher than diverse kinds of quenchers for biopolymers fluorescence (2.0 × 10^{10} M^{-1} s^{-1}) indicating the existence of static quenching mechanism [81].

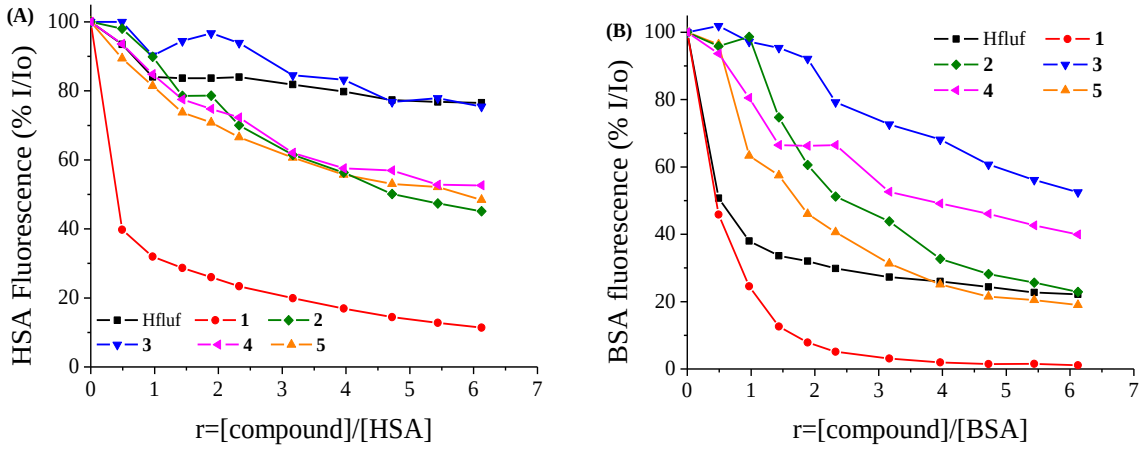

Fig. 5. (A) Plot of % relative fluorescence intensity at λ_{em} = 351 nm (%) vs r (r =[complex]/[HSA]) forHfluf and complexes **1**–**5** (75% of the initial fluorescence intensity for Hfluf, 11% for **1**, 45% for **2**, 75% for **3**, 52% for **4** and 49% for **5**) in buffer solution (150 mM NaCl and 15 mM trisodium citrate at pH 7.0). (B) Plot of % relative fluorescence intensity at λ_{em} = 342 nm (%) vs r (r = [complex]/[BSA]) for Hfluf and complexes **1**–**5** (22% of the initial fluorescence intensity for Hfluf, 1% for **1**, 23% for **2**, 52% for **3**, 40% for **4** and 19% for **5**) in buffer solution (150 mM NaCl and 15 mM trisodium citrate at pH 7.0).

The values of the association binding constant (K) and the number of binding sites per albumin (n), as calculated from the Scatchard equation (Eq. (2)) and Scatchard plots [58] (Figs. S6 and S7), for all compounds are given in Table 5. The K values are relatively high with **1** having the highest K values for both albumins used. Comparison of the n values reveals that all complexes exhibit higher n values than free Hfluf. Comparing the affinity of the complexes for BSA and HSA (K values), it is obvious that all compounds with the exception of **3** show higher affinity for BSA than HSA. In any case, the binding constant of a compound to the albumin should be at optimum; it should be high enough to allow binding of the compound and its possible transfer but also not too high in order to be released upon arrival at its target. It is quite noteworthy all K values are in accordance being within an optimum range; they are high enough to allow the binding of the compounds to SA and they are

also quite below the association constant of one of the strongest known non-covalent bonds, i.e. the interaction of avidin with diverse ligands with a K value ≈ 10^{15} M^{-1}, suggesting a possible release from the serum albumin to the target cells [82].

Table 5. The SA binding constants and parameters derived for Hfluf complexes **1-5**.

HSA				
Compound	**K_{sv} (M^{-1})**	**k_q (M^{-1} s^{-1})**	**K (M^{-1})**	**n**
Hfluf	1.86(±0.21) x 10^4	1.86(±0.42) x 10^{12}	1.79 x 10^5	0.31
$[Cu_2(fluf)_4(dmf)_2]$ **1**	3.79(±0.16) x 10^5	3.79(±0.32) x 10^{13}	5.53 x 10^5	0.97
[Cu(fluf)(bipyam)Cl] **2**	7.11(±0.21) x 10^4	7.11(±0.41) x 10^{12}	5.44 x 10^4	1.12
[Cu(fluf)(phen)Cl] **3**	2.07(±0.27) x 10^4	2.07(±0.54) x 10^{12}	1.09 x 10^5	0.35
[Cu(fluf)(bipy)Cl] **4**	5.20(±0.28) x 10^4	5.20(±0.55) x 10^{12}	7.65 x 10^4	0.85
$[Cu(fluf)_2(py)_2]$ **5**	5.62(±0.25) x 10^4	5.62(±0.50) x 10^{12}	1.11 x 10^5	0.77
BSA				
Compound	**K_{sv} (M^{-1})**	**k_q (M^{-1} s^{-1})**	**K (M^{-1})**	**n**
Hfluf	1.83(±0.20) x 10^5	1.83(±0.40) x 10^{13}	1.06 x 10^6	0.81
$[Cu_2(fluf)_4(dmf)_2]$ **1**	5.07(±0.37) x 10^6	5.07(±0.74) x 10^{14}	1.61 x 10^6	1.03
[Cu(fluf)(bipyam)Cl] **2**	1.98(±0.09) x 10^5	1.98(±0.18) x 10^{13}	9.55 x 10^4	1.23
[Cu(fluf)(phen)Cl] **3**	6.09(±0.65) x 10^4	6.09(±1.29) x 10^{12}	3.14 x 10^4	1.27
[Cu(fluf)(bipy)Cl] **4**	8.24(±0.36) x 10^4	8.24(±0.71) x 10^{12}	8.74 x 10^4	0.99
$[Cu(fluf)_2(py)_2]$ **5**	2.55(±0.09) x 10^5	2.55(±0.17) x 10^{13}	1.75 x 10^5	1.09

3.4. Interaction with calf-thymus DNA

The potential anticancer and the antiinflammatory activity of the NSAIDs and their complexes may be related to their ability to interact with DNA [22,23]. Therefore, such studies are of increasing interest since their number so far is quite limited; complexes of oxicam NSAIDs bind to DNA via intercalation [23], while the interaction of DNA with the copper(II) complexes of naproxen, diclofenac (NSAIDs of the phenylalkanoic acids' group), mefenamic acid (belongs to the group of the anthralinic acid NSAIDs) and diflunisal (a salicylate derivative NSAID) as well as of cobalt(II) naproxenato or mefenamato complexes has been recently reported by our lab [7,8,25,31,39–41]. As it is known, transition metal complexes can bind to DNA via both covalent (replacement of a labile ligand of the complex by a nitrogen base of DNA, e.g. guanine N7) and/or noncovalent (intercalation, electrostatic or groove binding) interactions [7,8].

Hfluf and complexes **1**–**5** exhibit similar behavior upon their addition on CT DNA solution. The UV spectra of a CT DNA solution with standard concentration (9×10^{-5} M) have been recorded in the presence of a compound at different [complex]/[DNA] mixing ratios (r) and representatively for **1** are shown in Fig. 6(A). The decrease of the intensity at λ_{max} = 258 nm is accompanied by a red-shift of the λ_{max} up to 263 nm for all compounds, indicating that the interaction with CT DNA results in the direct formation of a new complex with double-helical CT DNA [83]. The observed hypochromism could be attributed to $\pi \rightarrow \pi^*$ stacking interaction between the aromatic chromophore (either from quinolone and/or the N,N´-donor ligands) of the complexes and DNA base pairs consistent with the intercalative binding mode [59], while the red-shift (bathochromism) may be considered an evidence of stabilization of CT DNA duplex [84].

In the UV spectrum of **5** (Fig. 6(B)), the band centred at 344 nm (band I) exhibits a significant hypochromism of ~40% suggesting tight binding to CT DNA probably by intercalation. Further addition of DNA results in a gradual elimination of this band. Additionally, the band at 290 nm (band II) presents a hyperchromism of up to 30% accompanied by a red-shift of 12 nm (up to 312 nm), suggesting tight binding and stabilization. A distinct isosbestic point at 336 nm appears upon addition of CT DNA. The behavior of Hfluf (band I (at 344 nm): hypochromism of 50%; band II (at 292 nm): hyperchromism ~40% and red-shift of 10 nm) and complex **4** (band I (at 314 nm and 302 nm): hypochromismof 75%; band II (at 260 nm): hyperchromism ~50% and red-shift of 20 nm) (Fig. S8) upon addition of CT-DNA is quite similar to **5**.

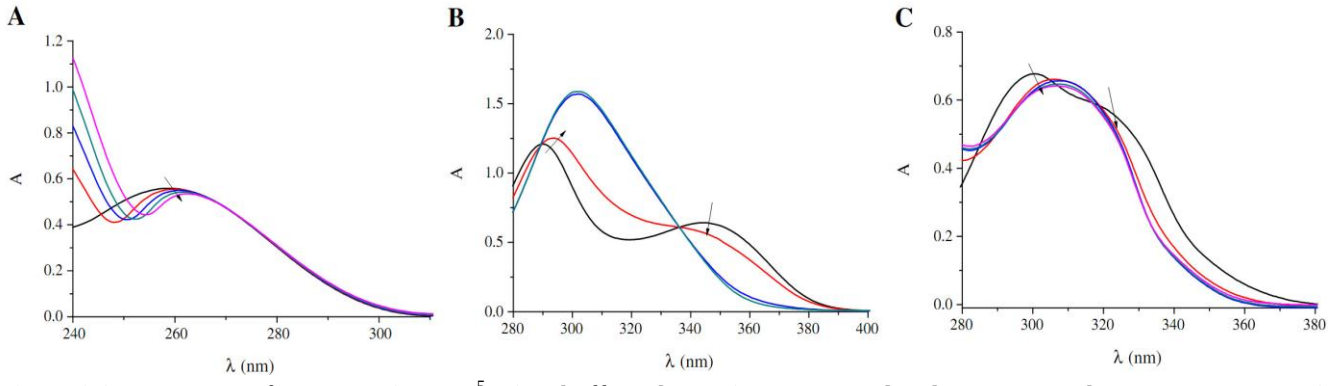

Fig. 6. (A) UV spectra of CT DNA (9×10^{-5} M) in buffer solution (150 mM NaCl and 15 mM trisodium citrate at pH 7.0) in the absence or presence of $[Cu_2(fluf)_4(DMF)_2]$, **1**. The arrow shows the changes upon increasing amounts of complex. (B) and (C) UV spectra of a DMSO solution (2×10^{-5} M) of (B) $[Cu(fluf)_2(py)_2]$, **5** and (C) [Cu(fluf)(bipyam)Cl], **2** in the presence of CT DNA at increasing amounts. The arrows show the changes upon increasing amounts of CT DNA.

In the UV spectrum of **2** (Fig. 6(C)), both bands centred at 300 nm and 320 nm present a hypochromism of ~10% and ~8%, respectively, while the first band is red-shifted towards 308 nm and the second band is rather eliminated. Quite similar is the behavior of complexes **1** (~8% hypochromism of the band at 300 nm accompanied by a bathochromism of 3 nm) and **3** (~6% hypochromism and a 2-nm bathochromism of the band at 297 nm) upon addition of increasing amounts of CT DNA (Fig. S8).

It should be noted that the exact mode of binding cannot be merely proposed by UV spectroscopic titration studies and the results collected from the UV titration experiments suggest that all compounds can bind to CT DNA [85]. The observed hypochromic effect may be considered as first evidence of tight binding to CT DNA probably by intercalation while the stabilization of the DNA duplex may be concluded as a result of the existence of a red-shift [86].

The values of the binding constant, K_b, of the compounds with CT DNA, as calculated by Eq. (3) [59] and the plots in Fig. S9, are given in Table 6. The K_b values are high and are of the same magnitude to that of the classical intercalator EB ($K_b = 1.23(\pm0.07) \times 10^5$ M^{-1}) [7,8]. The K_b values suggest a strong binding of the compounds to CT DNA [7,8], with complex **4** exhibiting the highest K_b values among the compounds. It is quite obvious that in most cases the coordination of flufenamic acid to Cu(II) results in an increase of the K_b value up to three to ten times.

Flufenamic acid exhibits the highest K_b value among the NSAIDs (naproxen, sodium diclofenac, mefenamic acid and tolfenamic acid) studied by our group so far [7,8,25,40]. Additionally, the flufenamato complexes **1**–**5** exhibit similarly the highest K_b values than the corresponding Cu(II) complexes with other NSAIDs as ligands [7,8,25].

Table 6. The DNA binding constants (K_b) and Stern-Volmer constants (K_{SV}) of EB-DNA fluorescence for Hfluf and complexes **1**–**5**.

Compound	K_b (M^{-1})	K_{sv} (M^{-1})
Hfluf	$2.70(\pm0.11) \times 10^5$	$6.34(\pm0.30) \times 10^5$
$[Cu_2(fluf)_4(dmf)_2]$ **1**	$9.44(\pm0.13) \times 10^5$	$5.97(\pm0.18) \times 10^5$
[Cu(fluf)(bipyam)Cl] **2**	$1.73(\pm0.34) \times 10^6$	$3.71(\pm0.11) \times 10^5$
[Cu(fluf)(phen)Cl] **3**	$2.53(\pm0.08) \times 10^5$	$6.97(\pm0.21) \times 10^5$
[Cu(fluf)(bipy)Cl] **4**	$2.68(\pm0.40) \times 10^6$	$10.53(\pm0.35) \times 10^5$
$[Cu(fluf)_2(py)_2]$ **5**	$7.80(\pm0.51) \times 10^5$	$3.35(\pm0.11) \times 10^5$

The cyclic voltammogram of **2** in DMSO solution exhibits two cathodic waves at −680 mV (E_{pc1}) and at −1200 mV (E_{pc2}, of lower current than E_{pc1}) which can show a two-step reduction of the species and they can be assigned to the process [Cu(II)] → [Cu(I)], and the formation of metallic copper [7,8,25,66], respectively, since Hfluf was found to be electrochemically inactive. The formation of Cu(I) is consistent with the metal-centered character of the LUMO orbitals of **2**–**5** (Table S9). These waves are followed by three non-reversible anodic waves at −550 mV (E_{pa1}), −45 mV (E_{pa2}) and +350 mV (E_{pa3}) which may be attributed to the oxidation processes

of metallic copper to [Cu(I)] (E_{pa1}) and [Cu(II)] (E_{pa2}) and of [Cu(I)] to [Cu(II)] (E_{pa3}). Complexes **1** and **3**–**5** have similar cyclic voltammograms in DMSO solution and the corresponding potentials are given in Table 7.

The investigation of metal–DNA interaction with electrochemical techniques is a useful complement to spectroscopic methods and may yield information about interactions with both the reduced and oxidized form of the metal. In general, when the metal ion or complex binds to DNA via intercalation, the electrochemical potential presents a positive shift, while, in the case of electrostatic interaction with DNA, the potential will shift to a negative direction. Moreover, if more potentials than one exist, a positive shift of E_{p1} and a simultaneous negative shift of E_{p2} may imply that the molecule can bind to DNA by both intercalation and electrostatic interaction [60,87].

Table 7. Cathodic and anodic potentials (in mV) for the redox couples of the complexes in DMSO solution and in DMSO/buffer solution in the absence or presence of CT DNA.

Complex	E_{pc1} [a]	E_{pc2} [a]	E_{pa1} [a]	E_{pa2} [a]	E_{pa3} [a]	$E_{pc(f)}$ [b]	$E_{pc(b)}$ [c]	ΔE_{pc} [d]	$E_{pa(f)}$ [b]	$E_{pa(b)}$ [c]	ΔE_{pa} [d]
$[Cu_2(fluf)_4(dmf)_2]$ **1**	–590	–1370	–80	+210	+465	–736	–715	+21	–510	–528	–18
[Cu(fluf)(bipyam)Cl] **2**	–680	–1200	–550	–45	+350	–743	–725	+18	–512	–525	–13
[Cu(fluf)(phen)Cl] **3**	–780	–1220	–550	+35	+410	–719	–660	+59	–516	495	+21
[Cu(fluf)(bipy)Cl] **4**	–600	–1130	–390	+30	+450	–737	–722	+15	–489	–483	+6
$[Cu(fluf)_2(py)_2]$ **5**	–650	–1210	–620	–45	+435	–788	–769	+19	–390	–360	+30

[a] $E_{pc/a}$ in DMSO solution

[b] $E_{pc/a}$ in DMSO/buffer in the absence of CT DNA ($E_{pc/a(f)}$)

[c] $E_{pc/a}$ in DMSO/buffer in the presence of CT DNA ($E_{pc/a(b)}$)

[d] $\Delta E_{pc/a} = E_{pc/a(b)} - E_{pc/a(f)}$

The redox couple for each complex in 1/2 DMSO/buffer solution studied upon addition of CT DNA as well as the shifts of the cathodic E_{pc} and anodic E_{pa} potentials are given in Table 7. No new redox peaks appeared after the addition of CT DNA to each complex; nevertheless, the observed decrease in current intensity (Fig. S10), attributed to an equilibrium mixture of free and DNA-bound complex to the electrode surface, may suggest the existence of an interaction between each complex and CT DNA [7,8,25,60,66]. All complexes 1–5 exhibit the same electrochemical behavior upon addition of CT DNA (Table 7) and, for increasing amounts of CT DNA, the cathodic and the anodic potentials exhibit predominantly a positive shift (ΔE_p =(−33)–(+59) mV) suggesting the existence of intercalation between the complexes and CT DNA bases [7,8,25,60].

The viscosity of DNA solution is sensitive to DNA length changes and its measurement upon addition of a compound may provide significant aid to clarify the interaction mode of a compound with DNA [8,39,40]. Viscosity measurements were carried out on CT DNA solutions upon addition of increasing amounts of the compounds. Fig. 7 shows that the addition of the complexes results in an increase in the relative viscosity of DNA. As known, the binding of a compound to DNA grooves via a partial and/or non-classic intercalation may provoke a bend or kink in the DNA helix subsequently resulting in a slight decrease of its effective length; in such a case, the viscosity of a DNA solution may show a slight decrease or may remain unchanged [88,89]. In the existence of classic intercalation, an insertion of the compound in between the DNA base pairs occurs leading to an increase in the separation of base pairs at intercalation sites in order to host the bound compound; therefore, the increase of the length of the DNA helix increases and the DNA viscosity exhibits an increase, the magnitude of which is usually in accordance to the strength of the interaction. In conclusion, the increase of the DNA viscosity observed upon addition of the compounds may be an evidence of the existence of an intercalative binding mode between DNA and each complex [8,39,40,88,89].

Ethidium bromide (EB = 3,8-Diamino-5-ethyl-6-phenylphenanthridinium bromide) is a typical indicator of intercalation [90] due to the intense fluorescence emission in the presence of CT DNA as a result of strong intercalation of the planar EB phenanthridine ring between adjacent base pairs on the double helix. Therefore, the changes observed in the fluorescence emission spectra of a solution containing EB bound to CT DNA may be used to study the interaction between DNA and other compounds, such as metal complexes, since the addition of a compound, capable to intercalate to DNA equally or more strongly than EB, should result in a quenching of the DNA-induced EB fluorescence emission [91]

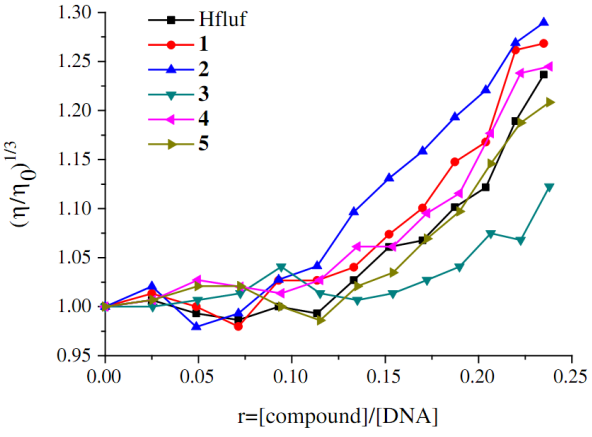

Fig. 7. Relative viscosity of CT DNA $(\eta/\eta_o)^{1/3}$ in buffer solution (150 mM NaCl and 15 mM trisodium citrate at pH 7.0) in the presence of Hfluf and complexes 1-5 at increasing amounts (r).

The emission spectra of EB bound to CT DNA in the absence and presence of each compound have been recorded for [EB] = 20 μM, [DNA] = 26 μM for increasing amounts of the compound. The addition of Hfluf or complexes **1**–**5** at diverse r values results in a significant decrease of the intensity of the emission band of the DNA–EB system at 592 nm (the final fluorescence is up to 21–45% of the initial EB–DNA fluorescence intensity for the complexes) indicating the competition of the complexes with EB in binding to DNA (Fig. 8). The observed significant quenching of DNA–EB fluorescence from the compounds suggests that they can displace EB from the DNA–EB complex, thus probably interacting with CT DNA by the intercalative mode [7,8,25,39,40]

The Stern–Volmer plots of DNA–EB (Fig. S11) illustrate that the quenching of EB bound to DNA by the compounds is in good agreement (R = 0.99) with the linear Stern–Volmer equation (Eq. (4)) [7,8,60]. The values (Table 6) of the Stern–Volmer constant (K_{SV}) as obtained by Stern–Volmer plots of DNA–EB (Fig. S11) show that the compounds can bind tightly to the DNA [7,8,25,39,40]. Flufenamic acid and its complexes **1**–**5** exhibit high KSV values in comparison to those of the NSAIDs (naproxen, sodium diclofenac, mefenamic acid) and their corresponding Cu(II) complexes studied by our group so far [7,8,25].

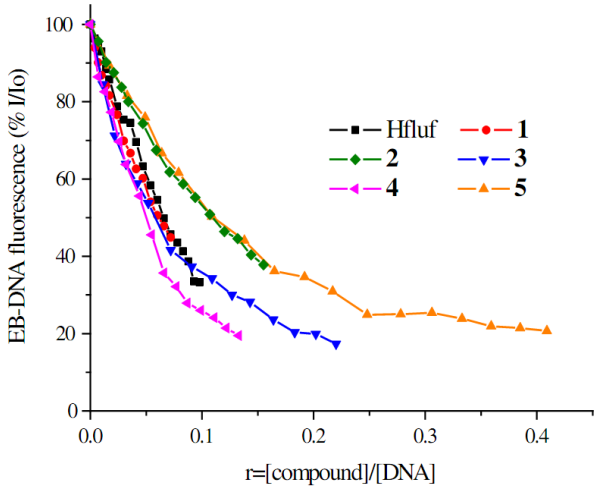

Fig. 8. Plot of EB-DNA relative fluorescence intensity (%I/Io) at λ_{em} = 592 nm vs r (r = [compound]/[DNA]) in buffer solution (150 mM NaCl and 15 mM trisodium citrate at pH 7.0) in the presence of Hfluf or complexes **1**–**5** (quenching up to 33% of the initial EB-DNA fluorescence for Hfluf, 45% for **1**, 38% for **2**, 17% for **3**, 19% for **4** and 21% for **5**).

3.5. Antioxidant capacity

The antioxidant activity of NSAIDs and their complexes may be related to their potential anticancer and antiinflammatory activity since free radicals play an important role in the inflammatory process. The NSAIDs with a broad spectrum of activity can also act either as inhibitors of free radical production or as radical scavengers [92]. Therefore, compounds possessing antioxidant properties could potentially have a crucial role

against inflammation and, thus, lead to potentially effective drugs. In this context, the potential antioxidant ability of Hfluf and complexes **1**–**5** has been evaluated in regard to DPPH, ABTS and hydroxyl radical scavenging ability and has been compared to that of well-known antioxidant agents e.g. NDGA, BHT and trolox. Compounds exhibiting DPPH radical scavenging activity are of increasing interest since DPPH scavenging activity is closely related to antiageing, anticancer and antiinflammatory activity [61]. Therefore, these antioxidants may offer protection in rheumatoid arthritis and inflammation and lead to potentially effective drugs. DPPH is a stable free radical presenting a strong absorption band at 517 nm. When antioxidants donate protons to DPPH radical, the initial absorbance of DPPH solution decreases. The scavenging activity of all compounds was not found to be time-dependent since no significant changes were observed after 20-min and 60-min measurements (Table 8). In general, the compounds present low to moderate reducing ability of DPPH radical with the complexes showing higher DPPH radical scavenging activity than free flufenamic acid. The complexes present similar scavenging activity of the DPPH radical to that found for a series of copper(II) complexes with the NSAIDs mefenamic acid and naproxen as ligands [7,39].

The scavenging activity of the ABTS radical cation ($ABTS^{\bullet+}$) may be related to the magnitude of the total antioxidant activity of the compounds [31]. The ABTS radical scavenging activity of the compounds was moderate to high in comparison to that of the reference compound trolox. All complexes show higher scavenging activity of $ABTS^{\bullet+}$ than free flufenamic acid, although it is lower than that of trolox. These results (Table 9) are in agreement to DPPH and hydroxyl radical scavenging studies revealing that complex 3 exhibits the highest scavenging activity of the ABTS radical cation among the complexes. Similar scavenging activity of the ABTS radical has been recorded for Cu(II) mefenamato and naproxenato complexes [7,39].

Table 8. Interaction % with DPPH (RA%).

Compound	20 min, 0,1mM	60 min, 0,1 mM
Hfluf	7.36(±0.52)	9.74(±0.38)
$[Cu_2(fluf)_4(DMF)_2]$, **1**	20.64(±0.91)	22.38(±0.72)
[Cu(fluf)(bipyam)Cl], **2**	13.77(±0.79)	14.31(±0.87)
[Cu(fluf)(phen)Cl], **3**	22.46(±0.19)	26.52(±0.55)
[Cu(fluf)(bipy)Cl], **4**	9.48(±0.31)	10.01(±0.36)
$[Cu(fluf)_2(py)_2]$, **5**	12.53(±0.67)	11.39(±0.61)
NDGA	81.02 (±0.18)	82.60 (±0.17)
BHT	31.30 (±0.10)	60.00 (±0.38)

Table 9. Competition % with DMSO for hydroxyl radical ($^{\cdot}OH$%), % superoxide radical scavenging activity (ABTS%) and *in vitro* inhibition of soybean lipoxygenase (LOX) (IC_{50}, in μM).

Compound	**ABTS% 0.1mM**	**$^{\cdot}OH$% 0.1mM**	**LOX IC_{50} (μM)**
Hfluf	64.57(±0.43)	84.51(±0.52)	42.64(±0.43)
$[Cu_2(fluf)_4(DMF)_2]$, **1**	84.61(±0.82)	93.59(±0.33)	27.51(±0.90)
[Cu(fluf)(bipyam)Cl], **2**	71.59(±0.79)	83.92(±0.83)	38.62(±0.58)
[Cu(fluf)(phen)Cl], **3**	89.44(±0.57)	93.71(±0.29)	24.73(±0.76)
[Cu(fluf)(bipy)Cl], **4**	73.46(±1.23)	91.48(±0.82)	39.98(±0.44)
$[Cu(fluf)_2(py)_2]$, **5**	72.72(±0.60)	82.62(±0.42)	46.09(±0.28)
Trolox	91.80(±0.17)	82.80(±0.13)	nt [a]
Caffeic acid	nt [a]	nt [a]	600 (±0.3)

[a] nt = not tested

Hydroxyl radicals are among the most reactive oxygen species. During the inflammatory process, the superoxide anion radicals are generated by phagocytes at the inflamed site and are connected to other oxidizing species such as •OH [31]. Under these conditions, hydroxyl radical scavengers could serve as protectors activating the prostaglandin synthesis. The competition of Hfluf and its Cu(II) complexes with DMSO for OH• generated by the Fe^{3+}/ascorbic acid system expressed as percent inhibition of formaldehyde production has been used for the evaluation of their hydroxyl radical scavenging activity and the results are given in Table 9. All compounds present higher competition with DMSO (33 mM) at 0.1 mM for hydroxyl free radicals than the reference

compound trolox and is similar to previously reported Cu(II) complexes with mefenamic acid and naproxen [7,39]. Additionally, the complexes present higher competition with DMSO for hydroxyl radical than free flufenamic acid, with complexes 1 and 3 being the most active compounds.

The inhibitory activity of the compounds against soybean lipoxygenase has been also tested. Most LOX inhibitors are antioxidants or free radical scavengers [93] since lipoxygenation occurs via a carbon centred radical. A relationship between LOX inhibition and the ability of the inhibitors to reduce the Fe(III) at the active site to the catalytically inactive Fe(II) has been previously reported. LOXs contain a 'non-heme' iron per molecule in the enzyme active site as high-spin Fe(III) in the native state and the high-spin in the activated state Fe(III). Several LOX inhibitors are excellent ligands for Fe(III) and their mechanism of action is presumably related to its coordination with a catalytically crucial Fe(III) [93,94]. All compounds present significant inhibition against soybean lipoxygenase (Table 9), especially in relation to the reference compound caffeic acid (IC50 = 600 μM), with 3 being the most active compound against LOX (IC50 = 24.73(±0.76) μM). Complexes 1–5 present similar or better in vitro inhibition of soybean lipoxygenase than the corresponding Cu(II) mefenamato complexes reported by our lab [7].

In conclusion, the scavenging activity of all the compounds tested is moderate to high in some cases. Additionally, the complexes exhibit slightly higher scavenging activity than free flufenamic acid against the DPPH, hydroxyl and ABTS radicals. Furthermore, Cu(II), Co(II), Ni(II), Zn(II) and Pd(II) complexes with drugs or Schiff bases as ligands exhibited better antioxidant activity than the free corresponding ligands [31,95–99].

4. Conclusions

The synthesis and characterization of the neutral copper(II) complex with the non-steroidal antiinflammatory drug flufenamic acid in the presence of the O-donor ligand N,N-dimethylformamide or a N-donor heterocyclic ligand 2,2′-bipyridylamine, 1,10-phenanthroline, 2,2′-bipyridine or pyridine has been achieved. The presence of DMF results in a dinuclear copper(II) complex with a paddlewheel arrangement while the presence of the N-donor ligands leads to the formation of mononuclear copper(II) complexes where the flufenamato ligands are bound via carboxylato oxygen atoms. The crystal structures of the complexes $[Cu_2(fluf)_4(DMF)_2]$, **1** and [Cu(fluf)(bipyam)Cl], **2** have been determined by X-ray Crystallography.

Density functional calculations (CAM-B3LYP/LANL2DZ/6-31G**) were employed to determine the structure of complexes **2**–**5**. A good agreement between the computed geometry of complex **2** and its crystal structure was found. According to DFT calculations, complexes **3** and **4** have a distorted square pyramidal geometry similar to that of **2**, while complex **5** can be optimized in an octahedral structure as observed for other related pyridine derivatives [25,28]. Time-dependent DFT calculations of doublet–doublet transitions have shown that the lowest-energy band in the absorption spectrum of **2**–**5** has a mixed d-d/LMCT character. Flufenamic acid and all complexes studied show good quenching ability of the BSA and HSA fluorescence and tight binding affinity to these proteins giving relatively high binding constants.

UV spectroscopy studies and viscosity measurements have revealed the ability of the complexes to bind to CT DNA. The binding strength of the complexes with CT DNA calculated with UV spectroscopic titrations have shown that [Cu(fluf)(bipy)Cl] exhibits the highest Kb value among the complexes examined, which is even higher than the Kb value of EB. Competitive binding studies with EB have revealed the ability of the complexes to displace the typical intercalator EB from the EB–CT DNA complex indicating intercalation as a possible mode of their interaction with CT DNA. The intercalative binding mode has been also confirmed by viscosity measurements of CT DNA solutions in the presence of the complexes as well as by cyclic voltammetry studies. Additionally, complexes **1**–**5** exhibit higher K_b values than previously reported Cu(II) complexes with the NSAIDs mefenamic acid, naproxen and diclofenac as ligands.

All compounds have been tested *in vitro* for their antioxidant, free radical scavenging activity and inhibitory activity on soybean lipoxygenase. They exhibit low DPPH radical scavenging activity and significantly high scavenging activity against hydroxyl free radicals and superoxide radicals. The compounds present significant inhibition against soybean lipoxygenase. Complex **3** is the most active scavenger of all radicals tested and the most potent LOX inhibitor.

Abbreviations

ABTS	2,2′-azinobis-(3-ethylbenzothiazoline-6-sulfonic acid) radical cation
BHT	butylated hydroxytoluene
bpy	2,2′-bipyridine
bipyam	2,2′-bipyridylamine
BSA	bovine serum albumin
COX	cyclo-oxygenase
CT	calf-thymus
DFT	density function theory
DMF	N,N-dimethylformamide
DMSO	dimethylsulfoxide
DPPH	1,1-diphenyl-picrylhydrazyl
EB	ethidium bromide, 3,8-diamino-5-ethyl-6-phenylphenanthridinium bromide
EDDM	electron density difference map
G09	Gaussian 09
Hdifl	diflunisal
Hfluf	flufenamic acid, N-(3-[trifluoromethyl]phenyl)anthranilic acid
Hnap	naproxen
HAS	human serum albumin
LMCT	ligand-to-metal charge transfer
LOX	soybean lipoxygenase
Nadicl	sodium diclofenac
NDGA	nordihydroguaiaretic acid
NSAID	non-steroidal antiinflammatory drug
phen	1,10-phenathroline
py	pyridine
SA	serum albumin
sh	shoulder
TEAP	tetraethylammonium perchlorate
Vs	very strong
Δ	$\nu_{asym}(CO_2)-\nu_{sym}(CO_2)$

Acknowledgments

This research has been co-financed by the European Union (European Social Fund-ESF) and Greek national funds through the Operational Program "Education and Lifelong Learning" of the National Strategic Reference Framework (NSRF)—Research Funding Program: Archimides III. L.S. was supported by the MICINN of Spain with the Ramón y Cajal Fellowship RYC-2011-07787. We thank the members of COST Action CM1105 for stimulating discussions.

Appendix A. Supplementary material

CCDC-917180 and 917181 contain the supplementary crystallographic data for this paper. These data can be obtained free of charge via www.ccdc.cam.ac.uk/conts/retrieving.html (or from the Cambridge Crystallographic Data Centre, 12 Union Road, Cambridge CB21EZ, UK; fax: (+44) 1223-336-033; or deposit@ccde.cam.ac.uk).

References

[1] G. Crisponi, V.M. Nurchi, D. Fanni, C. Gerosa, S. Nemolato, G. Faa, Coord. Chem. Rev. 254 (2010) 876–889.

[2] J.E.Weder, C.T. Dillon, T.W. Hambley, B.J. Kennedy, P.A. Lay, J.R. Biffin, H.L. Regtop, N.M. Davies, Coord. Chem. Rev. 232 (2002) 95–126.

[3] J.A. Drewry, P.T. Gunning, Coord. Chem. Rev. 255 (2011) 459–472.
[4] B.M. Rode, Y. Suwannachot, Coord. Chem. Rev. 190–192 (1999) 1085–1099.
[5] M.E. Katsarou, E.K. Efthimiadou, G. Psomas, A. Karaliota, D. Vourloumis, J. Med. Chem. 51 (2008) 470–478.
[6] E.K. Efthimiadou, H. Thomadaki, Y. Sanakis, C.P. Raptopoulou, N. Katsaros, A. Scorilas, A. Karaliota, G. Psomas, J. Inorg. Biochem. 101 (2007) 64–73.
[7] F. Dimiza, S. Fountoulaki, A.N. Papadopoulos, C.A. Kontogiorgis, V. Tangoulis, C.P. Raptopoulou, V. Psycharis, A. Terzis, D.P. Kessissoglou, G. Psomas, Dalton Trans. 40 (2011) 8555–8568.
[8] F. Dimiza, F. Perdih, V. Tangoulis, I. Turel, D.P. Kessissoglou, G. Psomas, J. Inorg. Biochem. 105 (2011) 476–489.
[9] E.K. Efthimiadou, Y. Sanakis, M. Katsarou, C.P. Raptopoulou, A. Karaliota, N. Katsaros, G. Psomas, J. Inorg. Biochem. 100 (2006) 1378–1388.
[10] G. Psomas, A. Tarushi, Y. Sanakis, E.K. Efthimiadou, C.P. Raptopoulou, N. Katsaros, J. Inorg. Biochem. 100 (2006) 1764–1773.
[11] M. Ruiz, L. Perello, J. Server-Carrio, R. Ortiz, S. Garcia-Granda, M.R. Diaz, E. Canton, J. Inorg. Biochem. 69 (1998) 231–239.
[12] A.M. Ramadan, J. Inorg. Biochem. 65 (1997) 183–189.
[13] C.P. Duffy, C.J. Elliott, R.A. O'Connor, M.M. Heenan, S. Coyle, I.M. Cleary, K. Kavanagh, S. Verhaegen, C.M. O'Loughlin, R. NicAmhlaoibh, M. Clynes, Eur. J. Cancer 34 (1998) 1250–1259.
[14] A.R. Amin, P. Vyas, M. Attur, J. Leszczynskapiziak, I.R. Patel, G. Weissmann, S.B. Abramson, Proc. Natl. Acad. Sci. 92 (1995) 7926–7930.
[15] D.H. Woo, I. Han, G. Jung, Life Sci. 75 (2004) 2439–2449.
[16] K. Kim, J. Yoon, J.K. Kim, S.J. Baek, T.E. Eling, W.J. Lee, J. Ryu, J.G. Lee, J. Lee, J. Yoo, Biochem. Biophys. Res. Commun. 325 (2004) 1298–1303.
[17] W.J.Wechter, E.D. Murray, D. Kantoci, D.D. Quiggle, D.D. Leipold, K.M. Gibson, J.D. McCracken, Life Sci. 66 (2000) 745–753.
[18] M.L. Smith, G. Hawcroft, M.A. Hull, Eur. J. Cancer 36 (2000) 664–674.
[19] L. Klampfer, J. Cammenga, H.G. Wisniewski, S.D. Nimer, Blood 93 (1999) 2386–2394.
[20] A. Inoue, S. Muranaka, H. Fujita, T. Kanno, H. Tamai, K. Utsumi, Free Radic. Biol. Med. 37 (2004) 1290–1299.
[21] M. Barbaric, M. Kralj, M. Marjanovic, I. Husnjak, K. Pavelic, J. Filipovic-Grcic, D. Zorc, B. Zorc, Eur. J. Med. Chem. 42 (2007) 20–29.
[22] T. Zhang, T. Otevrel, Z.Q. Gao, Z.P. Gao, S.M. Ehrlich, J.Z. Fields, B.M. Boman, Cancer Res. 61 (2001) 8664–8667.
[23] S. Roy, R. Banerjee, M. Sarkar, J. Inorg. Biochem. 100 (2006) 1320–1331.
[24] D. Kovala-Demertzi, A. Theodorou, M.A. Demertzis, C.P. Raptopoulou, A. Terzis, J. Inorg. Biochem. 65 (1997) 151–157.
[25] S. Fountoulaki, F. Perdih, I. Turel, D.P. Kessissoglou, G. Psomas, J. Inorg. Biochem. 105 (2011) 1645–1655.
[26] S. Lorinc, M. Koman, M. Melnik, J. Moncol, D. Ondrusova, Acta Crystallogr. E60 (2004) m590–m592.
[27] C. Dendrinou-Samara, D.P. Kessissoglou, G.E. Manoussakis, D. Mentzafos, A. Terzis, J. Chem. Soc. Dalton Trans. (1990) 959–965.
[28] A.L. Abuhijleh, J. Inorg. Biochem. 55 (1994) 255–262.
[29] J.E. Weder, T.W. Hambley, B.J. Kennedy, P.A. Lay, D. MacLachlan, R. Bramley, C.D. Delfs, K.S. Murray, B. Moubaraki, B. Warwick, J.R. Biffin, H.L. Regtop, Inorg. Chem. 38 (1999) 1736–1744; P. Kogerler, P.A.M. Williams, B.S. Parajon-Costa, E.J. Baran, L. Lezama, T. Rojo, A. Muller, Inorg. Chim. Acta 268 (1998) 239–248.
[30] A.E. Underhill, S.A. Bougourd, M.L. Flugge, S.E. Gale, P.S. Gomm, J. Inorg. Biochem. 52 (1993) 139–144.

[31] F. Dimiza, A.N. Papadopoulos, V. Tangoulis, V. Psycharis, C.P. Raptopoulou, D.P. Kessissoglou, G. Psomas, Dalton Trans. 39 (2010) 4517–4528.
[32] H. Yau, G. Baranauskas, Marco Martina, J. Physiol. 588 (2010) 3869–3882.
[33] Y. Chi, K. Li, Q. Yan, S. Koizumi, L. Shi, S. Takahashi, Y. Zhu, H. Matsue, M. Takeda, M. Kitamura, J. Yao, J. Pharmacol. Exp. Ther. 339 (2011) 257–266.
[34] F. Pena, M.A. Parkis, A.K. Tryba, J.M. Ramirez, Neuron 43 (2004) 105–117.
[35] P. Poronnik, M.C. Ward, D.I. Cook, FEBS Lett. 296 (1992) 245–248.
[36] M. Ottolia, L. Toro, Biophys. J. 67 (1994) 2272–2279.
[37] G. Facchin, M.H. Torre, E. Kremer, O.E. Piro, E.J. Baran, Z. Anorg. Allg. Chem. 624 (1998) 2025–2028.
[38] A. Tarushi, F. Kastanias, V. Psycharis, C.P. Raptopoulou, G. Psomas, D.P. Kessissoglou, Inorg. Chem. 51 (2012) 7460–7462.
[39] F. Dimiza, A.N. Papadopoulos, V. Tangoulis, V. Psycharis, C.P. Raptopoulou, D.P. Kessissoglou, G. Psomas, J. Inorg. Biochem. 107 (2012) 54–64.
[40] S. Tsiliou, L.-A. Kefala, F. Perdih, I. Turel, D.P. Kessissoglou, G. Psomas, Eur. J. Med. Chem. 48 (2012) 132–142.
[41] A. Tarushi, X. Totta, C. Raptopoulou, V. Psycharis, G. Psomas, D.P. Kessissoglou, Dalton Trans. 41 (2012) 7082–7091.
[42] P. Christofis, M. Katsarou, A. Papakyriakou, Y. Sanakis, N. Katsaros, G. Psomas, J. Inorg. Biochem. 99 (2005) 2197–2210.
[43] C. Tan, J. Liu, H. Li, W. Zheng, S. Shi, L. Chen, L. Ji, J. Inorg. Biochem. 102 (2008) 347–358.
[44] Rigaku/MSC, CrystalClear, Rigaku/MSC Inc., The Woodlands, Texas, USA, 2005.
[45] G.M. Sheldrick, SHELXS-97: Structure Solving Program, University of Göttingen, Germany, 1997.
[46] G.M. Sheldrick, SHELXL-97: Crystal Structure Refinement Program, University of Göttingen, Germany, 1997.
[47] M.J. Frisch, G.W. Trucks, H.B. Schlegel, G.E. Scuseria, M.A. Robb, J.R. Cheeseman, G. Scalmani, V. Barone, B. Mennucci, G.A. Petersson, H. Nakatsuji, M. Caricato, X. Li, H.P. Hratchian, A.F. Izmaylov, J. Bloino, G. Zheng, J.L. Sonnenberg, M. Hada, M. Ehara, K. Toyota, R. Fukuda, J. Hasegawa, M. Ishida, T. Nakajima, Y. Honda, O. Kitao, H. Nakai, T. Vreven, J.A. Montgomery Jr., J.E. Peralta, F. Ogliaro, M. Bearpark, J.J. Heyd, E. Brothers, K.N. Kudin, V.N. Staroverov, R. Kobayashi, J. Normand, K. Raghavachari, A. Rendell, J.C. Burant, S.S. Iyengar, J. Tomasi, M. Cossi, N. Rega, J.M. Millam, M. Klene, J.E. Knox, J.B. Cross, V. Bakken, C. Adamo, J. Jaramillo, R. Gomperts, R.E. Stratmann, O. Yazyev, A.J. Austin, R. Cammi, C. Pomelli, J.W. Ochterski, R.L. Martin, K. Morokuma, V.G. Zakrzewski, G.A. Voth, P. Salvador, J.J. Dannenberg, S. Dapprich, A.D. Daniels, O. Farkas, J.B. Foresman, J.V. Ortiz, J. Cioslowski, D.J. Fox, Gaussian 09, Revision B.01, Gaussian, Inc., Wallingford CT, 2009.
[48] M. Casida, C. Jamorski, K.C. Casida, D.R. Salahub, J. Chem. Phys. 108 (1998) 4439–4449.
[49] R. Stratmann, G.E. Scuseria, M.J. Frisch, J. Chem. Phys. 109 (1998) 8218–8224.
[50] T. Yanai, D. Tew, N. Handy, Chem. Phys. Lett. 393 (2004) 51–57.
[51] P. Hay, W.R. Wadt, J. Chem. Phys. 82 (1985) 270–273.
[52] A.D. McLean, G.S. Chandler, J. Chem. Phys. 72 (1980) 5639–5648.
[53] D.M. York, M. Karplus, J. Phys. Chem. A 103 (1999) 11060–11079.
[54] N.M. O'Boyle, A.L. Tenderholt, K.M. Langner, J. Comput. Chem. 29 (2008) 839–845.
[55] E.F. Pettersen, T.D. Goddard, C.C. Huang, G.S. Couch, D.M. Greenblatt, E.C. Meng, T.E. Ferrin, J. Comput. Chem. 25 (2004) 1605–1612.
[56] J.R. Lakowicz, Principles of Fluorescence Spectroscopy, 3rd ed. Plenum Press, New York, 2006.
[57] J.R. Lakowicz, G. Weber, Biochemistry 12 (1973) 4161–4170.
[58] S. Wu, W. Yuan, H. Wang, Q. Zhang, M. Liu, K. Yu, J. Inorg. Biochem. 102 (2008) 2026–2034.
[59] A.M. Pyle, J.P. Rehmann, R. Meshoyrer, C.V. Kumar, N.J. Turro, J.K. Barton, J. Am. Chem. Soc. 111 (1989) 3053–3063.
[60] G. Psomas, J. Inorg. Biochem. 102 (2008) 1798–1811.
[61] C. Kontogiorgis, D. Hadjipavlou-Litina, J. Enzyme Inhib. Med. Chem. 18 (2003) 63–69.

[62] R. Re, N. Pellegrini, A. Proteggente, A. Pannala, M. Yang, C. Rice-Evans, Free Radic. Biol. Med. 26 (1999) 1231–1237.
[63] K.R. Prabhakar, V.P. Veerapur, P. Bansal, V. Kumar, M. Reddy, A. Barik, B.K. Reddy, P. Reddanna, K.I. Priyadarsini, M.K. Unnikrishnan, Bioorg. Med. Chem. 14 (2006) 7113–7120.
[64] K. Nakamoto, Infrared and Raman Spectra of Inorganic and Coordination Compounds, Part B: Applications in Coordination, Organometallic, and Bioinorganic Chemistry, 6th ed. Wiley, New Jersey, 2009.
[65] B.J. Hathaway, in: G. Wilkinson (Ed.), Comprehensive Coordination Chemistry, vol. 5, Pergamon Press, Oxford, 1987, pp. 533–773.
[66] P. Zivec, F. Perdih, I. Turel, G. Giester, G. Psomas, J. Inorg. Biochem. 117 (2012) 35–47.
[67] B.J. Hathaway, Struct. Bond. (Berlin) 14 (1973) 49–67.
[68] A.W. Addison, T.N. Rao, J. Reedijk, J. van Rijn, G.C. Verchoor, J. Chem. Soc. Dalton Trans. (1984) 1349–1356.
[69] C. Castellari, G. Feroci, S. Ottani, Acta Crystallogr. C 55 (1999) 907–910.
[70] S. Youngme, K. Chinnakali, S. Chantrapromma, H. Fun, Acta Crystallogr. C55 (1999) 899–901.
[71] R.E. Marsh, Acta Crystallogr. B61 (2005) 359.
[72] Y. Wang, N. Okabe, Inorg. Chim. Acta 358 (2005) 3407–3416.
[73] F. Ugozzoli, A.M.M. Lanfredi, N. Marsich, A. Camus, Inorg. Chim. Acta 256 (1997) 1–7.
[74] N. Okabe, A. Tsuji, M. Yodoshi, Acta Crystallogr. E63 (2007) m2162.
[75] N. Okabe, A. Tsuji, M. Yodoshi, Acta Crystallogr. E63 (2007) m2108–m2109.
[76] Y. Wang, G. Lin, J. Hong, T. Lu, L. Li, N. Okabe, M. Odoko, Inorg. Chim. Acta 362 (2009) 377–384.
[77] N. Okabe, A. Tsuji, M. Yodoshi, Acta Crystallogr. E63 (2007) m1756–m1757.
[78] S. Youngme, A. Cheansirisomboon, C. Danvirutai, N. Chaichit, C. Pakawatchai, G.A. van Albada, J. Reedijk, Inorg. Chem. Commun. 9 (2006) 973–977.
[79] R. Carballo, B. Covelo, N. Fernandez-Hermida, A.B. Lago, E.M. Vazquez-Lopez, Z. Anorg. Allg. Chem. 633 (2007) 1791–1795.
[80] C. Tan, J. Liu, H. Li, W. Zheng, S. Shi, L. Chen, L. Ji, J. Inorg. Biochem. 102 (2008) 347–358.
[81] Y. Wang, H. Zhang, G. Zhang, W. Tao, S. Tang, J. Lumin. 126 (2007) 211–218.
[82] V. Rajendiran, R. Karthik, M. Palaniandavar, H. Stoeckli-Evans, V.S. Periasamy, M.A. Akbarsha, B.S. Srinag, H. Krishnamurthy, Inorg. Chem. 46 (2007) 8208–8221.
[83] Q. Zhang, J. Liu, H. Chao, G. Xue, L. Ji, J. Inorg. Biochem. 83 (2001) 49–55.
[84] E.C. Long, J.K. Barton, Acc. Chem. Res. 23 (1990) 271–273.
[85] A. Jancso, L. Nagy, E. Moldrheim, E. Sletten, J. Chem. Soc. Dalton Trans. (1999) 1587–1594.
[86] G. Pratviel, J. Bernadou, B. Meunier, Adv. Inorg. Chem. 45 (1998) 251–262.
[87] M.T. Carter, M. Rodriguez, A.J. Bard, J. Am. Chem. Soc. 111 (1989) 8901–8911.
[88] J.L. Garcia-Gimenez, M. Gonzalez-Alvarez, M. Liu-Gonzalez, B. Macias, J. Borras, G. Alzuet, J. Inorg. Biochem. 103 (2009) 923–934.
[89] J. Liu, H. Zhang, C. Chen, H. Deng, T. Lu, L. Li, Dalton Trans. (2003) 114–119.
[90] W.D. Wilson, L. Ratmeyer, M. Zhao, L. Strekowski, D. Boykin, Biochemistry 32 (1993) 4098–4104.
[91] S. Dhar, M. Nethaji, A.R. Chakravarty, J. Inorg. Biochem. 99 (2005) 805–812.
[92] R. Cini, G. Giorgi, A. Cinquantini, C. Rossi,M. Sabat, Inorg. Chem. 29 (1990) 5197–5200.
[93] K. Muller, Arch. Pharm. 327 (1994) 3–19.
[94] J. Van der Zee, T.E. Eling, R.P. Mason, Biochemistry 28 (1989) 8363–8367.
[95] S.B. Bukhari, S. Memona, M.M. Tahir, M.I. Bhanger, J. Mol. Struct. 892 (2008) 39–46.
[96] Z.D. Petrovic, D. Hadjipavlou-Litina, V.P. Petrovic, J. Mol. Liq. 144 (2009) 55–58.
[97] E. Pontiki, D. Hadjipavlou-Litina, A.T. Chaviara, C.A. Bolos, Bioorg. Med. Chem. Lett. 16 (2006) 2234–2237.
[98] Z. Liu, B.Wang, Z. Yang, Y. Li, D. Qin, T. Li, Eur. J. Med. Chem. 44 (2009) 4477–4484.
[99] K.C. Skyrianou, F. Perdih, A.N. Papadopoulos, I. Turel, D.P. Kessissoglou, G. Psomas, J. Inorg. Biochem. 105 (2011) 1273–1285.